

# Fatigue Testing of Galvanized and Ungalvanized Socket Connections

PUBLICATION NO. FHWA-HRT-14-066

SEPTEMBER 2014



U.S. Department of Transportation  
**Federal Highway Administration**

Research, Development, and Technology  
Turner-Fairbank Highway Research Center  
6300 Georgetown Pike  
McLean, VA 22101-2296

## FOREWORD

Wind-induced vibration of ancillary structures that support signs and lights for traffic operations has been known to cause fatigue cracks that sometimes lead to collapse. Since approximately 1990, many researchers have called attention to this problem, and prior research has led to many changes in the American Association of State Highway Transportation Officials *Standard Specifications for Structural Supports for Highway Signs, Luminaires, and Traffic Signals*. One particular detail of interest is the ring-to-tube connection used at the base of poles, commonly referred to as a socket connection. Typically, these connections have demonstrated comparatively reduced fatigue resistance. Much of the data on socket connection fatigue reveals that poles which had been galvanized have reduced fatigue strength. However, not all owners galvanize their structures, meaning the fatigue resistance of non-galvanized structures is being unnecessarily discounted. This project specifically addressed the difference in socket connection fatigue resistance between galvanized and ungalvanized poles. This report will assist stakeholders, including State transportation departments, researchers, consultants, and industry representatives, with the design and review of ancillary sign structures.

Jorge E. Pagán-Ortiz  
Director, Office of Infrastructure  
Research and Development

### Notice

This document is disseminated under the sponsorship of the U.S. Department of Transportation in the interest of information exchange. The U.S. Government assumes no liability for the use of the information contained in this document.

The U.S. Government does not endorse products or manufacturers. Trademarks or manufacturers' names appear in this report only because they are considered essential to the objective of the document.

### Quality Assurance Statement

The Federal Highway Administration (FHWA) provides high-quality information to serve Government, industry, and the public in a manner that promotes public understanding. Standards and policies are used to ensure and maximize the quality, objectivity, utility, and integrity of its information. FHWA periodically reviews quality issues and adjusts its programs and processes to ensure continuous quality improvement.

**TECHNICAL REPORT DOCUMENTATION PAGE**

1. Report No. FHWA-HRT-14-066	2. Government Accession No.	3. Recipient's Catalog No.	
4. Title and Subtitle Fatigue Testing of Galvanized and Ungalvanized Socket Connections		5. Report Date September 2014	
		6. Performing Organization Code:	
7. Author(s) Justin M. Ocel, Ph.D., P.E.		8. Performing Organization Report No.	
9. Performing Organization Name and Address Federal Highway Administration Bridge and Foundation Engineering Team (HRDI-40) Turner-Fairbank Highway Research Center 6300 Georgetown Pike McLean, VA 22101		10. Work Unit No.	
		11. Contract or Grant No.	
12. Sponsoring Agency Name and Address Office of Infrastructure Research and Development Federal Highway Administration 6300 Georgetown Pike McLean, VA 22101-2296		13. Type of Report and Period Covered	
		14. Sponsoring Agency Code HRDI-40	
15. Supplementary Notes			
16. Abstract The fatigue resistance of welded traffic signal support structure details is an ongoing research topic being addressed at multiple universities primarily through state funding mechanisms. Fatigue problems with these structures have plagued multiple states, and a handful of collapses are identified in the open literature. Some premature failures have been hypothesized to have been caused by cracking in the zinc metal bath during galvanizing. This led to a fatigue testing matrix of socket connection geometries in a galvanized and ungalvanized state. Specimens were attained from two different pole manufacturers and fabricated using their own techniques. This report describes how the specimens were tested along with the results showing the difference in fatigue life between galvanized and ungalvanized structures. Generally, the galvanized specimens showed a one-category reduction in fatigue life versus identical specimens that were not galvanized.			
17. Key Words Sign pole, fatigue, socket connection, galvanizing, wind vibration, tube-to-plate, ancillary structure		18. Distribution Statement No restrictions. This document is available to the public through the National Technical Information Service, Springfield, VA 22161. <a href="http://www.ntis.gov">http://www.ntis.gov</a>	
19. Security Classif. (of this report) Unclassified	20. Security Classif. (of this page) Unclassified	21. No. of Pages 43	22. Price N/A

## SI\* (MODERN METRIC) CONVERSION FACTORS

### APPROXIMATE CONVERSIONS TO SI UNITS

Symbol	When You Know	Multiply By	To Find	Symbol
<b>LENGTH</b>				
in	inches	25.4	millimeters	mm
ft	feet	0.305	meters	m
yd	yards	0.914	meters	m
mi	miles	1.61	kilometers	km
<b>AREA</b>				
in <sup>2</sup>	square inches	645.2	square millimeters	mm <sup>2</sup>
ft <sup>2</sup>	square feet	0.093	square meters	m <sup>2</sup>
yd <sup>2</sup>	square yard	0.836	square meters	m <sup>2</sup>
ac	acres	0.405	hectares	ha
mi <sup>2</sup>	square miles	2.59	square kilometers	km <sup>2</sup>
<b>VOLUME</b>				
fl oz	fluid ounces	29.57	milliliters	mL
gal	gallons	3.785	liters	L
ft <sup>3</sup>	cubic feet	0.028	cubic meters	m <sup>3</sup>
yd <sup>3</sup>	cubic yards	0.765	cubic meters	m <sup>3</sup>
NOTE: volumes greater than 1000 L shall be shown in m <sup>3</sup>				
<b>MASS</b>				
oz	ounces	28.35	grams	g
lb	pounds	0.454	kilograms	kg
T	short tons (2000 lb)	0.907	megagrams (or "metric ton")	Mg (or "t")
<b>TEMPERATURE (exact degrees)</b>				
°F	Fahrenheit	5 (F-32)/9 or (F-32)/1.8	Celsius	°C
<b>ILLUMINATION</b>				
fc	foot-candles	10.76	lux	lx
fl	foot-Lamberts	3.426	candela/m <sup>2</sup>	cd/m <sup>2</sup>
<b>FORCE and PRESSURE or STRESS</b>				
lbf	poundforce	4.45	newtons	N
lbf/in <sup>2</sup>	poundforce per square inch	6.89	kilopascals	kPa

### APPROXIMATE CONVERSIONS FROM SI UNITS

Symbol	When You Know	Multiply By	To Find	Symbol
<b>LENGTH</b>				
mm	millimeters	0.039	inches	in
m	meters	3.28	feet	ft
m	meters	1.09	yards	yd
km	kilometers	0.621	miles	mi
<b>AREA</b>				
mm <sup>2</sup>	square millimeters	0.0016	square inches	in <sup>2</sup>
m <sup>2</sup>	square meters	10.764	square feet	ft <sup>2</sup>
m <sup>2</sup>	square meters	1.195	square yards	yd <sup>2</sup>
ha	hectares	2.47	acres	ac
km <sup>2</sup>	square kilometers	0.386	square miles	mi <sup>2</sup>
<b>VOLUME</b>				
mL	milliliters	0.034	fluid ounces	fl oz
L	liters	0.264	gallons	gal
m <sup>3</sup>	cubic meters	35.314	cubic feet	ft <sup>3</sup>
m <sup>3</sup>	cubic meters	1.307	cubic yards	yd <sup>3</sup>
<b>MASS</b>				
g	grams	0.035	ounces	oz
kg	kilograms	2.202	pounds	lb
Mg (or "t")	megagrams (or "metric ton")	1.103	short tons (2000 lb)	T
<b>TEMPERATURE (exact degrees)</b>				
°C	Celsius	1.8C+32	Fahrenheit	°F
<b>ILLUMINATION</b>				
lx	lux	0.0929	foot-candles	fc
cd/m <sup>2</sup>	candela/m <sup>2</sup>	0.2919	foot-Lamberts	fl
<b>FORCE and PRESSURE or STRESS</b>				
N	newtons	0.225	poundforce	lbf
kPa	kilopascals	0.145	poundforce per square inch	lbf/in <sup>2</sup>

\*SI is the symbol for the International System of Units. Appropriate rounding should be made to comply with Section 4 of ASTM E380.  
(Revised March 2003)

## TABLE OF CONTENTS

<b>INTRODUCTION.....</b>	<b>1</b>
<b>SPECIMENS .....</b>	<b>1</b>
<b>TESTING METHODS .....</b>	<b>5</b>
<b>FATIGUE TESTING .....</b>	<b>5</b>
<b>ULTIMATE LOAD TESTING .....</b>	<b>5</b>
<b>MATERIAL CHARACTERIZATION .....</b>	<b>6</b>
<b>EXPERIMENTAL DATA.....</b>	<b>9</b>
<b>MATERIAL CHARACTERIZATION .....</b>	<b>9</b>
Chemistry of Galvanizing .....	10
Fatigue Testing.....	11
Ultimate Load Testing .....	18
<b>SUMMARY .....</b>	<b>23</b>
<b>APPENDIX: PICTURES OF FRACTURES .....</b>	<b>25</b>
<b>REFERENCES.....</b>	<b>37</b>

## LIST OF FIGURES

Figure 1. Illustration. Detailing of specimens from each fabricator .....	3
Figure 2. Illustration. Schematic of socket connection testing frame.....	7
Figure 3. Illustration. ASTM E8 “plate-type” specimen .....	8
Figure 4. Graph. S-N plot of fabricator 1 fatigue data.....	15
Figure 5. Graph. S-N plot of fabricator 2 fatigue data.....	16
Figure 6. Photo. Peening evidence on Specimen 1U3 .....	17
Figure 7. Graph. Moment versus displacement of test 1 .....	19
Figure 8. Graph. Moment versus displacement of test 2 .....	20
Figure 9. Graph. Moment versus displacement of test 3 .....	20
Figure 10. Graph. Moment versus displacement of test 4 .....	21
Figure 11. Photo. Specimen 1U1 fracture surface .....	25
Figure 12. Photo. Specimen 1U2 fracture surface .....	26
Figure 13. Photo. Specimen 1U3 fracture surface .....	26
Figure 14. Photo. Specimen 1U4 fracture surface .....	27
Figure 15. Photo. Specimen 1U5 fracture surface .....	27
Figure 16. Photo. Specimen 1U6 fracture surface .....	28
Figure 17. Photo. Specimen 1G2 fracture surface .....	28
Figure 18. Photo. Specimen 1G3 fracture surface .....	29
Figure 19. Photo. Specimen 1G4 fracture surface .....	29
Figure 20. Photo. Specimen 1G5 fracture surface .....	30
Figure 21. Photo. Specimen 1G6 fracture surface .....	30
Figure 22. Photo. Specimen 2U1 fracture surface .....	31
Figure 23. Photo. Specimen 2U2 fracture surface .....	31
Figure 24. Photo. Specimen 2U3 fracture surface .....	32
Figure 25. Photo. Specimen 2U4 fracture surface .....	32
Figure 26. Photo. Specimen 2U5 fracture surface .....	33
Figure 27. Photo. Specimen 2U6 fracture surface .....	33
Figure 28. Photo. Specimen 2G1 fracture surface .....	34
Figure 29. Photo. Specimen 2G2 fracture surface .....	34
Figure 30. Photo. Specimen 2G3 fracture surface .....	35
Figure 31. Photo. Specimen 2G4 fracture surface .....	35
Figure 32. Photo. Specimen 2G5 fracture surface .....	36
Figure 33. Photo. Specimen 2G6 fracture surface .....	36

## LIST OF TABLES

Table 1. Fabricator 1 material data .....	9
Table 2. Fabricator 2 material data .....	10
Table 3. Galvanized coating chemistries .....	11
Table 4. Fatigue results of fabricator 1 specimens .....	13
Table 5. Fatigue results of fabricator 2 specimens .....	14
Table 6. Static testing matrix .....	19





## INTRODUCTION

Fatigue of structural supports for overhead signs, traffic signals, and highmast light poles has received focused attention from researchers in the last 25 years because of failures that have been reported in welded details. The likely precipitating event was the close consecutive collapse of two cantilevered signal structures in Michigan in 1990, which resulted in property damage, injuries, and one fatality.<sup>(1)</sup> These lightweight, flexible structures are often susceptible to vibration from wind phenomena such as galloping, vortex shedding, and wind gusts. The dynamic response tends to excite the lower modes of vibration, and with very low damping ratios, large numbers of loading cycles quickly accumulate. These wind-induced vibrations can ultimately lead to fatigue cracking at welded details in the structure. One type of welded connection with poor fatigue resistance is the pole-to-base plate welds that often follow socket connection detailing practice. To make a socket connection, a hole is cut out of the base plate with a slightly larger diameter than the outside diameter of the pole. The tube is partially slid into the base plate, and a perimeter fillet weld adjoins the two pieces, essentially creating a hollow section with a thick stiffening ring welded to the end. The socket connection is the preferred connection method between a pole and a foundation because it can be quickly fabricated.

Fatigue testing of socket connection details began in the early 1980s at Lehigh University but had a resurgence once the 2001 American Association of State Highway Transportation Officials (AASHTO) *Standard Specifications for Structural Supports for Highway Signs, Luminaires, and Traffic Signals* was published.<sup>(2,3)</sup> The 2001 specifications were the first to include fatigue design, which had not been considered in prior editions. In-service structures that historically never had fatigue issues were not meeting the 2001 fatigue provisions. To be compatible with the new provisions, States, designers, and fabricators had to drastically increase pole diameters and wall thickness to comply with the 2001 fatigue provisions. In response to concerns with this situation, several research projects addressed the fatigue resistance of traffic signal structure details, mainly with socket connection details. Some of these projects were conducted at the University of Wyoming, University of Texas–Austin (UT–Austin), Lehigh University, Purdue University, and the University of Minnesota. (See references 4–9.) One of the larger fatigue testing studies published in 2011 (National Cooperative Highway Research Program Project 10-70) included only galvanized details, which provided the lower bound of fatigue resistance based on the research of Koenigs.<sup>(6,8)</sup> This decision ultimately led to specification changes that neglected any increased fatigue resistance of structures that are not galvanized.

## SPECIMENS

The desired specimen utilized a round tube with an 18-inch outside diameter at the socket connection, 0.25-inch wall thickness, 2-inch-thick base plate, and a 6-bolt, 2-inch-diameter anchor rod arrangement on a 24-inch-diameter bolt circle. A construction drawing was created and sent to two different fabricators. They were asked to provide shop drawings of how the specimen could best be fabricated using their typical processes. Four differences arose between the two manufacturers. Each used different weld profiles, and each had their own galvanizing sources. Fabricator 2 could not make perfectly round poles and instead made round-like tubes by press-braking a flat plate with multiple bends. Fabricator 1 made the tubes from ASTM A595 steel; whereas, fabricator 2 bent ASTM A572 Gr.65 material into a tube. Figure 1 illustrates the

detailing of the desired specimen and each fabricator's shop drawing. Twelve specimens were acquired from each fabricator. Six were in an unfinished state, and six were hot-dip galvanized.

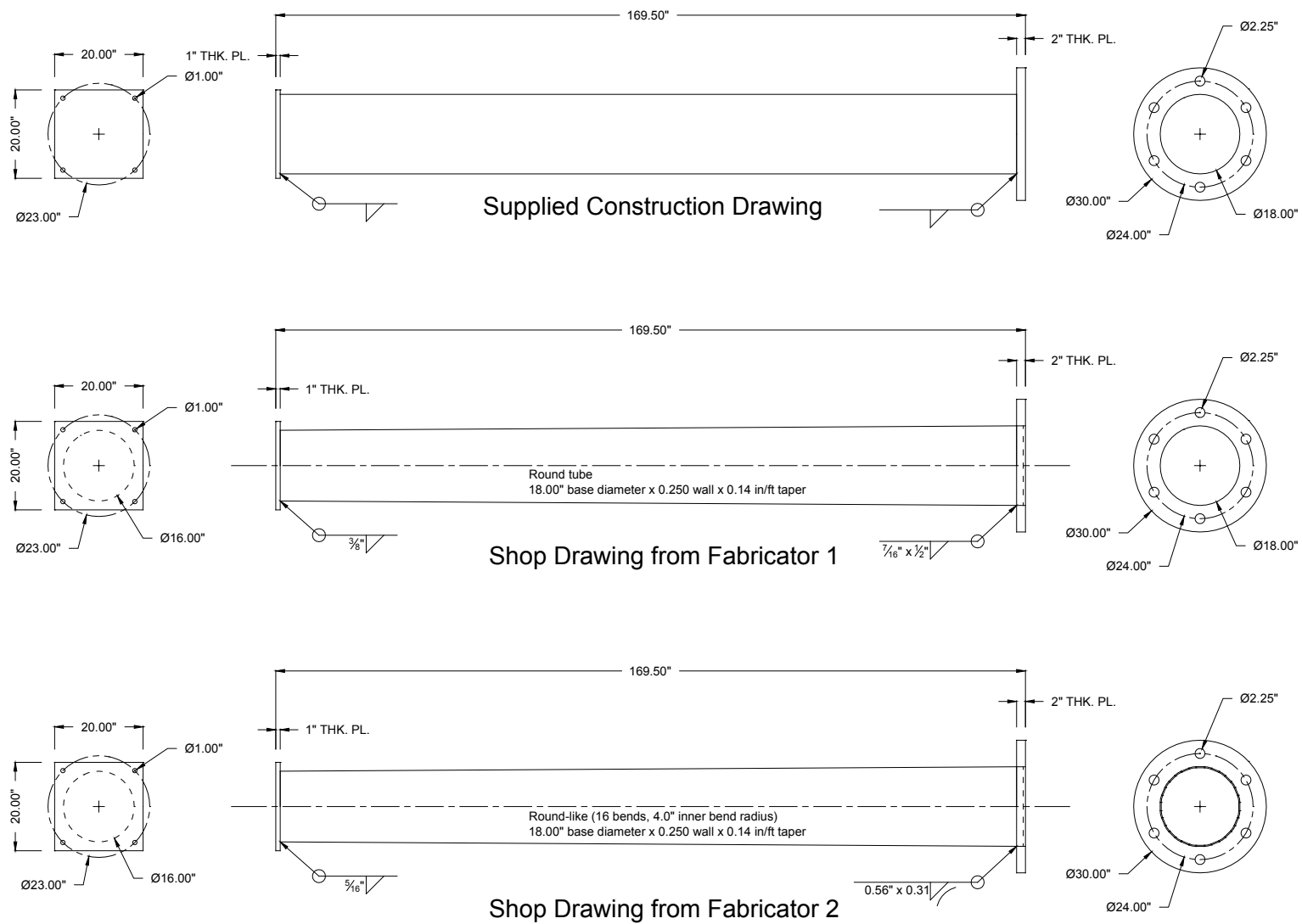


**Figure 1. Illustration. Detailing of specimens from each fabricator.**



## TESTING METHODS

Fatigue testing was performed in a specially fabricated load frame shown in figure 2. The methodology was based on a concept first performed at UT–Austin by bolting two pole specimens to a loading box and then simply supporting the ends of poles and loading through the loading box.<sup>(6)</sup> For this project, the loading box was replaced with a large concrete block. The block had dimensions of 45 by 45 by 72 inches and was cast of concrete, thus weighing just over 12.6 kips. Six 2-inch by 4.5UNC B7 threaded rods passed through the entire length of the block and stuck out approximately 12 inches on each side. These threaded rods were used to bolt the pole specimens to the loading block with double-nut moment joints. The leveling nuts were spaced approximately one rod diameter off the concrete surface. The benefit of using the concrete block to load the poles was to accurately recreate the boundary conditions typical for socket connections bolted to a concrete foundation. The threaded rods were orientated such that one rod was at the point of maximum bending stress. Specimens were randomly selected for installation, and the installation orientation was also randomized, that is, no attempt was made to orient the tube seam weld into a beneficial configuration. Since the socket connections had a six-bolt pattern and the support ends had a four-bolt pattern, the specimen could be installed in only one of two orientations.

### FATIGUE TESTING

During fatigue cycling the actuator would pull up on the loading block to induce a dead load stress in the pole. The actuator would cycle in between loads of 11.63 and 15.73 kips. This equated to a calculated mean (dead load) of approximately 19.3 ksi because the round and round-like poles had slightly different moments of inertia. This load range induced a stress range of 5.85 ksi in the fabricator 1 specimens and 5.73 ksi in the fabricator 2 specimens. The specimens were cycled either in load or displacement control. When running in load control, the actuator could not cycle faster than 0.8 Hz without going unstable. To expedite testing, most cycling occurred in displacement control with the actuator cycling at about 2.7 Hz, which was near the natural frequency of the system. The peak displacement targets were attained when the actuator had come to operating temperature and running in load control. Once a day, the displacement targets were verified and altered accordingly. However, once one of the two cycling specimens started to grow a crack, the test was run exclusively in load control to ensure a consistent stress range. Throughout the testing program, two poles never simultaneously reached failure; one pole always failed before another.

The specimens were cycled at a low stress range to ensure the threaded rods were below their fatigue threshold. If the threaded rods had failed, a new loading block would have to be fabricated. This was the fundamental drawback to using this concrete loading block versus the steel loading box used in the UT–Austin research.

### ULTIMATE LOAD TESTING

Strength tests were performed on eight of the cracked pole sections. This was done to assess the remaining capacity of the cracked section, for instance, as a way to determine the risk associated with keeping a knowingly cracked pole in service. The same loading system was used in the strength tests as in the fatigue tests, except the tests were run monotonically until failure.

Two parameters were investigated in the strength tests: loading rate and temperature. The loading rate was analyzed in terms of the applied displacement from the actuator. The first two tests were conducted at 0.002 and 0.04 inches/s at room temperature. The first represented a true static loading rate and the second represented a rate closer to that of a wind loading event on a pole. The second two tests were conducted at 0.02 and 0.2 inches/s at -30 °F, which is the AASHTO Zone 2 lowest anticipated service temperature. To attain -30 °F, a rigid foam box was built around each connection and injected with liquid nitrogen through a solenoid valve controlled by a temperature controller and a thermocouple attached to the base plate of the connection. The difference in the loading rates was accidental. The first tests were performed using old analog controllers, while the second tests were run with digital controllers, which were upgraded through the duration of the project. The different loading rates were an artifact of not understanding the new digital controller functionality. All the poles tested statically were from fabricator 2.

The actuator had only a 6-inch stroke. In the tests to failure, the system had to be unloaded frequently, spacers had to be added at the support, and the system reloaded until failure occurred. Failure was defined as attaining a peak load or a fracture of the cross section.

## **MATERIAL CHARACTERIZATION**

Tensile coupon testing was used to characterize the steel plate used to make the specimen supplied by each of the fabricators. Testing was performed according to the ASTM E8 Specification.<sup>(10)</sup> The coupons were machined according to the schematic shown in figure 3. All pretest measurements and markings were also performed in accordance with ASTM E8.

Testing was performed on a four-post universal testing machine with hydraulic wedge grips and a 220 kip capacity. The testing machine was controlled with a digital controller. Strain measurements were made using a clip-on extensometer with a 1-inch measurement range but fitted with an extension bar to measure strain over an 8.000-inch gauge length.

Specimens were initially loaded at a rate of 0.0003 inch/s. Once the specimen had yielded, the static yield was attained by pausing the loading for a period of 90 seconds in three locations along the yield plateau. Once strain hardening had begun, the loading rate was gradually increased to 0.01 inch/s until the specimen fractured. Typically, it took approximately 20 min to fracture a specimen.

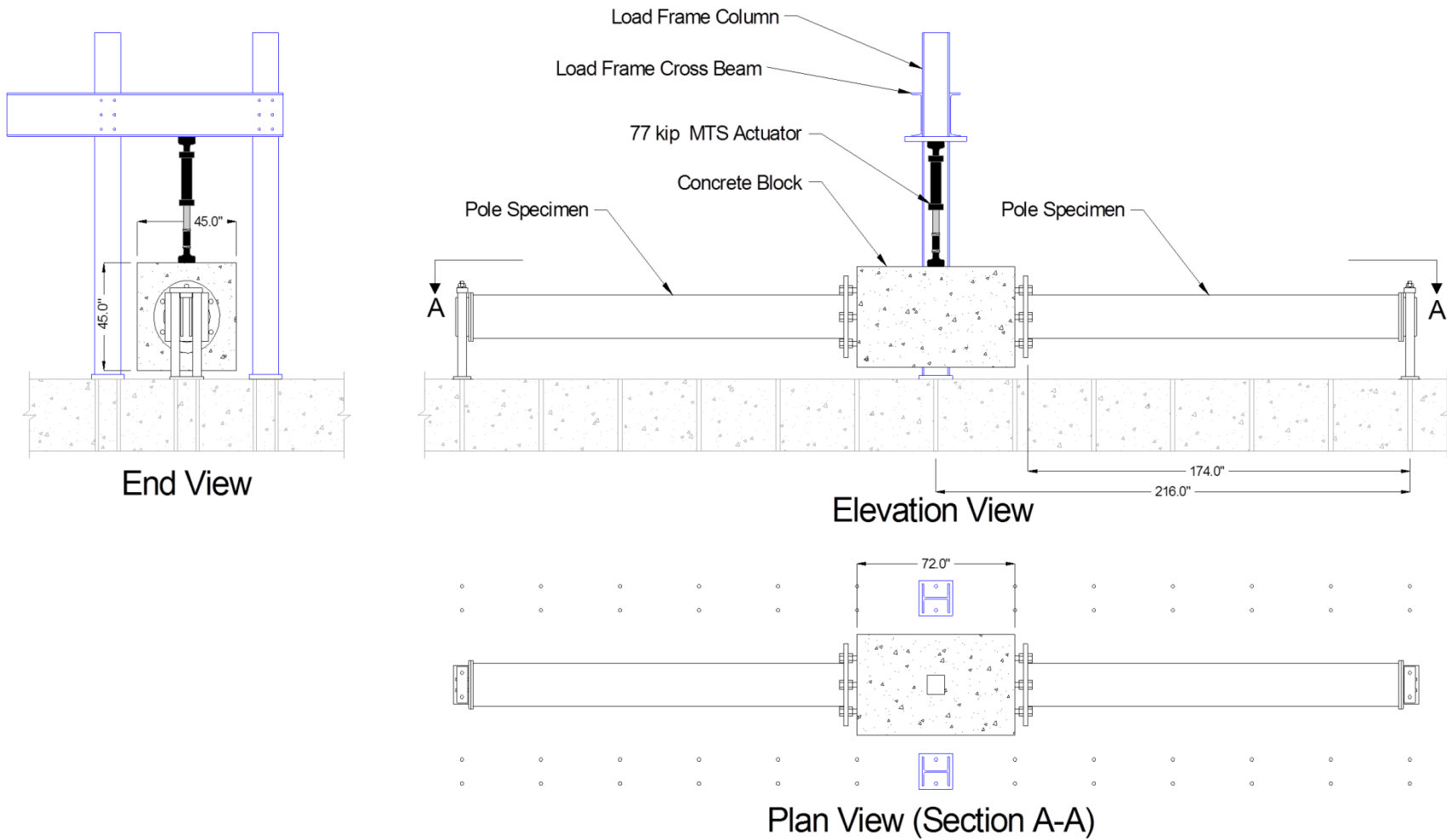


**Figure 2. Illustration. Schematic of socket connection testing frame.**

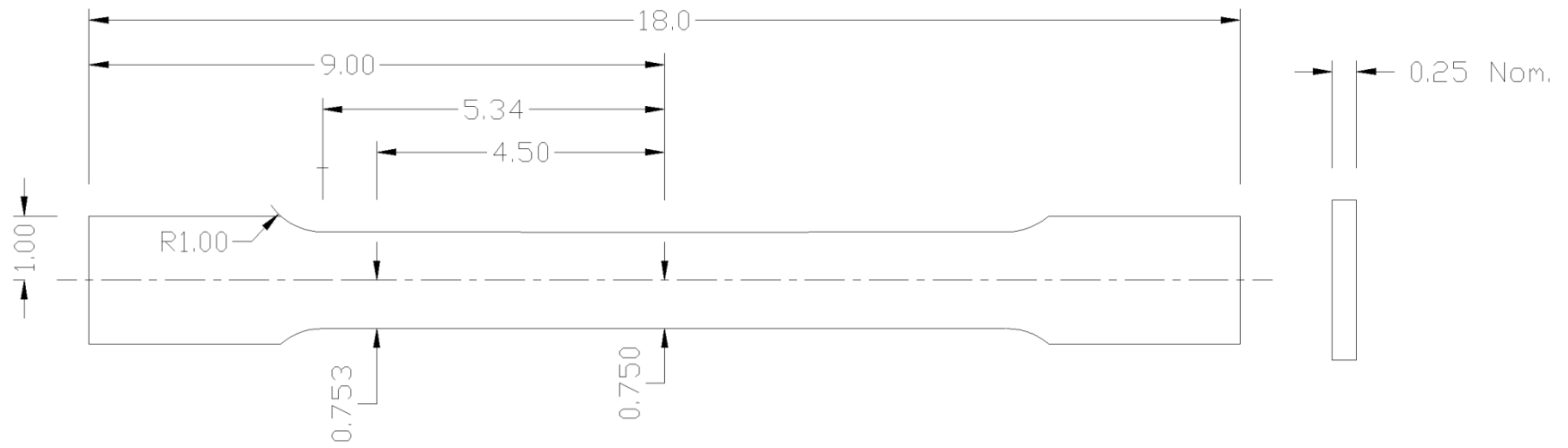


**Figure 3. Illustration. ASTM E8 "plate-type" specimen.**



## EXPERIMENTAL DATA

### MATERIAL CHARACTERIZATION

In total, 20 coupons were tested, five from each set of galvanized and bare specimens. Table 1 and table 2 show the results of testing for each of the fabrication sources. The averages for each set of specimens are shown in the bolded line. Fabricator 1 had average 0.2-percent yield strengths of 51.5 and 48.7 ksi for the respective galvanized and bare coupons. Fabricator 2 had average 0.2-percent yield strengths of 69.3 and 64.7 ksi for the respective galvanized and bare coupons.

**Table 1. Fabricator 1 material data.**

<b>Specimen ID</b>	<b>0.2% Offset Yield Stress (ksi)</b>	<b>Static Yield Stress (ksi)</b>	<b>Tensile Strength (ksi)</b>	<b>Elongation (percent)</b>	<b>Area Reduction (percent)</b>
Galv1	50.5	48.7	63.6	22	59
Galv2	52.5	49.8	64.8	20	64
Galv3	50.4	48.3	62.4	23	63
Galv4	51.3	49.2	63.7	22	62
Galv5	52.8	50.7	64.8	23	66
<b>Average</b>	<b>51.5</b>	<b>49.3</b>	<b>63.9</b>	<b>22</b>	<b>63</b>
Bare1	47.2	45.6	58.9	23	58
Bare2	48.8	47.3	58.9	26	57
Bare3	49.3	47.7	60.3	26	62
Bare4	49.3	47.9	61.5	27	56
Bare5 <sup>a</sup>	43.1	42.8	61.2	26	61
<b>Average<sup>b</sup></b>	<b>48.7</b>	<b>47.1</b>	<b>59.9</b>	<b>25</b>	<b>58</b>

<sup>a</sup> Indicates specimens where fracture occurred outside the original gauge length marks or was located less than 25 percent of the elongated gauge length from either of the original gauge length marks.

<sup>b</sup> Specimens failing ASTM acceptance criteria were not included in statistical analysis.

**Table 2. Fabricator 2 material data.**

<b>Specimen ID</b>	<b>0.2% Offset Yield Stress (ksi)</b>	<b>Static Yield Stress (ksi)</b>	<b>Tensile Strength (ksi)</b>	<b>Elongation (percent)</b>	<b>Area Reduction (percent)</b>
Galv1 <sup>a</sup>	69.1	67.5	76.0	14	55
Galv2	68.2	65.5	76.3	14	76
Galv3	66.7	64.7	73.5	15	73
Galv4	73.1	70.6	80.6	14	69
Galv5 <sup>a</sup>	72.9	70.5	79.9	15	85
<b>Average<sup>b</sup></b>	<b>69.3</b>	<b>66.9</b>	<b>76.8</b>	<b>14</b>	<b>73</b>
Bare1	65.4	62.5	75.6	16	74
Bare2	65.9	64.5	74.6	12	76
Bare3	63.3	61.4	74.0	15	71
Bare4	65.6	63.4	76.3	16	72
Bare5	63.5	61.9	74.3	15	76
<b>Average</b>	<b>64.7</b>	<b>62.7</b>	<b>75.0</b>	<b>15</b>	<b>74</b>

<sup>a</sup> Indicates specimens where fracture occurred outside the original gauge length marks or was located less than 25 percent of the elongated gauge length from either of the original gauge length marks.

<sup>b</sup> Specimens failing ASTM acceptance criteria were not included in statistical analysis.

### **Chemistry of Galvanizing**

Neither of the specimen fabricators would provide the chemistry of their zinc baths, pleading it was proprietary information. Therefore, a core plug was removed from four randomly selected specimens, two from each manufacturer. The core plugs were sent to a lab for chemical analysis of the zinc coating. Table 3 shows the results of the chemistry in terms of percent by weight. No conclusions will be drawn on the chemistry results, although elevated levels of some elements have been known to cause cracking. They are presented here for information purposes only.

**Table 3. Galvanized coating chemistries.**

<b>Element</b>	<b>1G5</b>	<b>1G6</b>	<b>2G6</b>	<b>2G5</b>
Copper	0.015	0.013	0.018	0.018
Cadmium	0.001	0.001	0.004	0.005
Aluminum	0.081	0.081	0.080	0.080
Magnesium	0.003	0.003	0.003	0.003
Lead	0.35	0.31	0.56	0.55
Tin	<0.001	<0.001	0.011	0.013
Iron	1.24	1.23	0.65	0.73
Nickel	0.016	0.017	0.078	0.077
Zinc	Balance	Balance	Balance	Balance

### **Fatigue Testing**

For this research, failure was considered a 12-inch-long crack around the perimeter of the tube. The UT–Austin researchers defined failure as a 10-percent decrease in the stiffness of the system. For this research the stiffness criterion was evaluated, but it was not believed to be accurate, since only one pole would fail at a time, while during the UT–Austin tests, poles would always fail in pairs. Generally once the crack was 12 inches long (21 percent of the perimeter), the remaining life was small in comparison to the cycles to reach failure. In addition, once the crack became that long, the stress range in each anchor rod around the intact portions of the pole would increase, thus increasing the risk that they could develop fatigue cracks themselves. The 12-inch crack length criterion was not strictly followed, particularly in the beginning of the testing with fabricator 1 specimens when the 10-percent stiffness reduction criteria was being evaluated. Initially the 10-percent stiffness decrease rule was used, but it was determined to be not working after the fourth specimen; then the 12-inch-long crack rule was adopted.

Table 4 and table 5 outline the fatigue data for the 24 socket connections tested. Specimens were assigned a 3-character, alphanumeric naming designation *xyz* where:

- *x* is 1 or 2 representing the two fabricators.
- *y* is either a U or G representing either unfinished or galvanized coatings.
- *z* represents the individual specimen (1 through 6).

Therefore, specimen 2G5 represents the fifth galvanized specimen from fabricator 2. Table 4 and table 5 also show the length of the crack on each tube’s perimeter at failure. The appendix contains photos of each fracture surface showing the crack’s shape, length, and area reported (figure 11 through figure 33).

An anomaly in the fatigue data requires further explanation. At one point in the program, Specimen 1U6 was being fatigue cycled along with Specimen 1G1. Specimen 1U6 had existing cracks from previous cycling, and Specimen 1G1 was virgin. After 616,158 cycles, there was an accidental overload applied to the system and evidence that the actuator applied approximately

32 kips of load to the system based on the peak/valley indicator on the controller. This overload destroyed the 1U6 specimen but caused no visible damage to the 1G1 specimen. The fact that Specimen 1G1 accumulated more than 15 million cycles with no cracks is not coincidental considering that the overload must have plastically deformed the tube at the weld toe, thus erasing the residual stresses from the welding and enhancing fatigue life.

Figure 4 and figure 5 plot the fatigue data along with the AASHTO S-N curves for fabricators 1 and 2, respectively. The colored, dashed lines represent the lower bound limit of the two data sets as the mean minus two standard deviations from linear regression analysis and an assumed slope of -3 to 1 on the log-log scale. The dashed blue line represents the ungalvanized specimens, and the dashed red line signifies the galvanized specimens.

For fabricator 1 the data are highly scattered for both the galvanized and ungalvanized specimens. For both specimen types, the lower bound resistance is similar and much less than Category E'. The scatter in the data can be explained by considering the preparation and quality of the socket weld from fabricator 1. Specimens with fatigue lives of more than 2 million cycles had welds with a low entry angle into the tube. In addition, evidence indicated that the weld toes were peened.

Figure 6 shows the peened surface of the weld from Specimen 1U3. (Note that the white line at the weld toe is residual developer from dye penetrant testing.) The speckled surface on the weld suggests that it was needle peened, and in some cases the weld toe was also treated. All of the fabricator 1 welds appear to have been needle peened, but the weld toes were not treated in all cases. The specimens with the lowest lives had equal leg welds and bad undercutting in some instances with cracks developing at multiple locations at each undercut.

The data from fabricator 2 are much more pronounced, showing the difference in fatigue strength between galvanized and ungalvanized specimens, with two distinct scatter bands for each specimen type. The lower bound of the ungalvanized specimens did plot slightly above Category E'; whereas, the galvanized specimens were much below Category E', similar in strength to the specimens made by fabricator 1.

**Table 4. Fatigue results of fabricator 1 specimens.**

<b>Specimen</b>	<b>Finish</b>	<b>Stress Range (ksi)<sup>a</sup></b>	<b>Cycles to Failure</b>	<b>Crack Length on Tube Perimeter (inches)</b>
1U1	Unfinished	5.85	2167227	6.90
1U2	Unfinished	5.85	1602406	7.59
1U3	Unfinished	5.85	3846508	6.19
1U4	Unfinished	5.85	8555356	8.59
1U5	Unfinished	5.85	924948	12.10
1U6	Unfinished	5.85	3835237 <sup>b</sup>	8.06
1G1	Galvanized	5.85	15015310 <sup>c</sup>	No crack
1G2	Galvanized	5.85	4461772	6.72
1G3	Galvanized	5.85	3067630	10.86
1G4	Galvanized	5.85	1229060	11.25
1G5	Galvanized	5.85	1360291	12.09
1G6	Galvanized	5.85	2928887	12.00

<sup>a</sup> Stress range calculated using a moment arm distance of 174 inches, moment of inertia of 549.14 inches, and an extreme fiber distance of 9 inches.

<sup>b</sup> The actuator accidentally full-scaled (possibly applied ~32 kips of load) and destroyed this specimen before the failure criterion was reached.

<sup>c</sup> Specimen was declared a runout. Extreme life was hypothesized to be from accidental overload when tested together with Specimen 1U6.

**Table 5. Fatigue results of fabricator 2 specimens.**

<b>Specimen</b>	<b>Finish</b>	<b>Stress Range (ksi)<sup>a</sup></b>	<b>Cycles to Failure</b>	<b>Crack Length on Tube Perimeter (inches)</b>
2U1	Unfinished	5.73	3738417	13.99
2U2	Unfinished	5.73	4873910	12.58
2U3	Unfinished	5.73	7000983	11.63
2U4	Unfinished	5.73	4411691	14.06
2U5	Unfinished	5.73	3409173	11.76
2U6	Unfinished	5.73	5631182	12.61
2G1	Galvanized	5.73	1171624	13.77
2G2	Galvanized	5.73	878218	12.68
2G3	Galvanized	5.73	639952	13.56
2G4	Galvanized	5.73	1864066	12.48
2G5	Galvanized	5.73	700310	12.64
2G6	Galvanized	5.73	748184	11.42

<sup>a</sup> Stress range calculated using a moment arm distance of 174 inches, moment of inertia of 561.61 inches, and an extreme fiber distance of 9.02 inches.

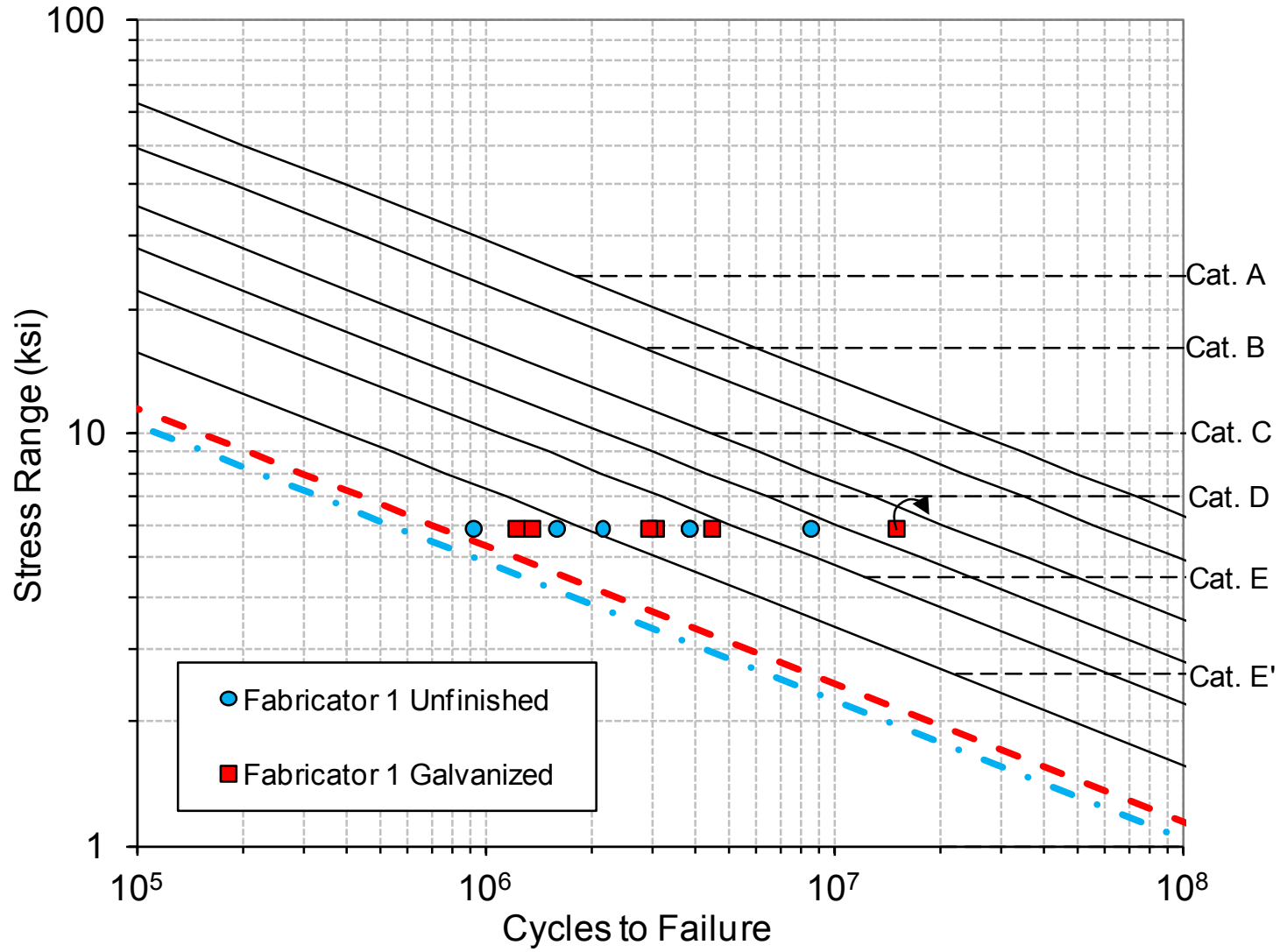


Figure 4. Graph. S-N plot of fabricator 1 fatigue data.

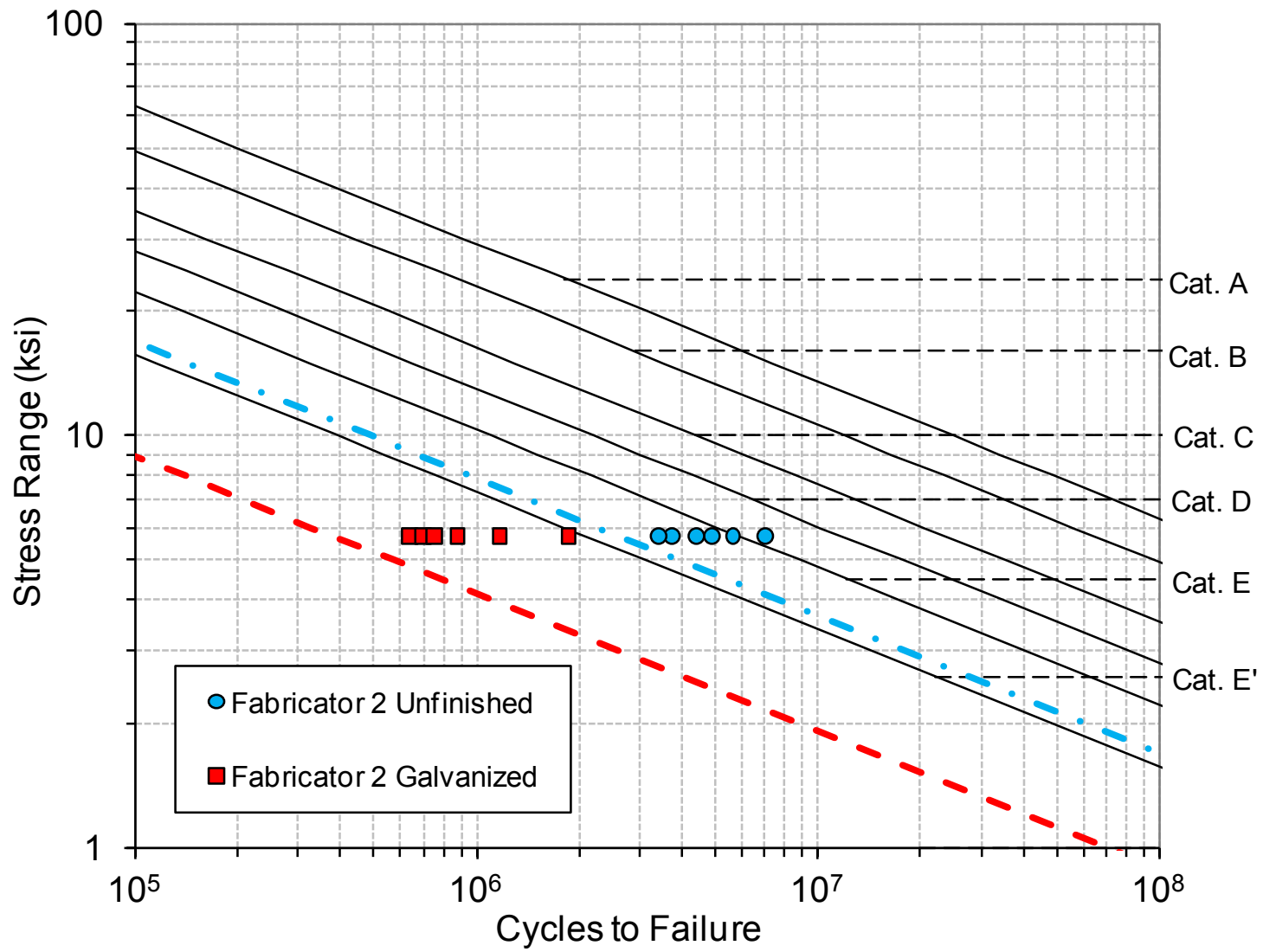
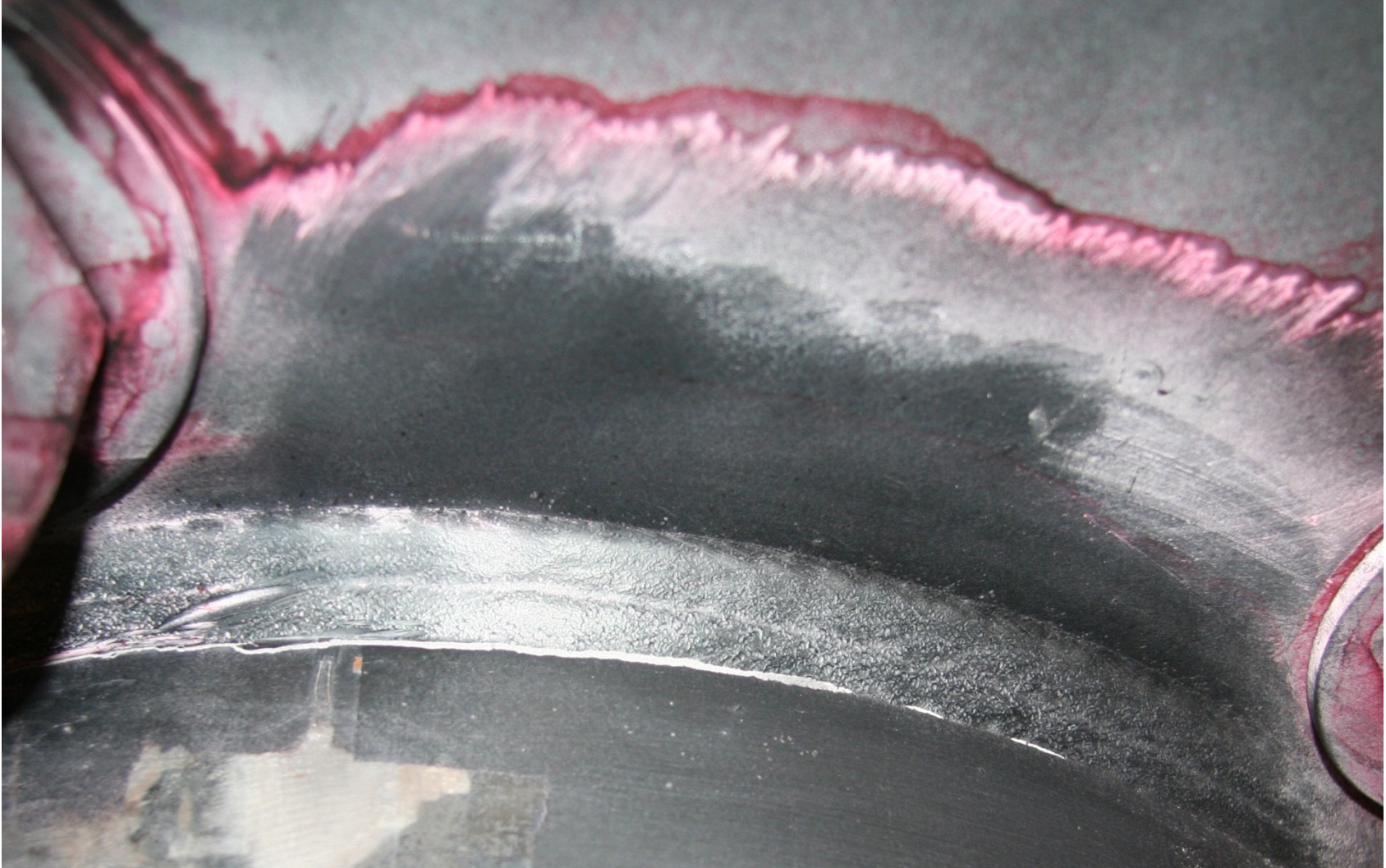


Figure 5. Graph. S-N plot of fabricator 2 fatigue data.





**Figure 6. Photo. Peening evidence on Specimen 1U3.**

## Ultimate Load Testing

The static tests were meant to be conducted to two different loading rates and two different temperatures. The two loading rates were meant to be extremely slow to represent static loading, and the faster rate was intended to represent a strain rate from a dynamic wind event. During the duration of the project, however, a new actuator control system was set up, and a mix-up occurred in interpreting the loading rates from one system to the next. Therefore, the rates do not necessarily represent the intention of the testing. Two temperatures were investigated: room temperature (approximately 70 °F) and the AASHTO Zone 2 lowest anticipated service temperature for fracture assessment (-30 °F).

Table 6 shows the matrix of tests together with the fatigue crack length, measured loading rate, and the peak moment attained for each test. For the mode of failure, in the two room temperature tests, the fatigue cracks extended in a ductile manner with through-thickness yielding of the tube. The two tests conducted at the cold temperature exhibited stable and ductile extension of the existing fatigue cracks with one exception. In test 3, one tube had a pop-in fracture where the fatigue crack suddenly extended 2 inches at a 45-degree angle relative to the fatigue crack propagation.

Figure 7 through figure 10 show the moment versus displacement plots for each of the four tests. In each plot, dashed and dotted lines indicate the plastic moments of the uncracked and cracked sections using the measured yield strength of the tube. The cracked section plastic modulus was calculated assuming a 12-inch-long crack on the outside perimeter of the tube. On average, the beginning crack lengths were 12 inches for the eight specimens tested. No attempt was made to calculate the cracked plastic section modulus for each tube individually.

The peak moments attained for each set of tubes were very close to the theoretical cracked section plastic moment capacity. This would indicate that if an owner did have a cracked pole in service, and could accurately assess the shape and length of the crack, a cracked plastic section analysis could be performed to determine if the pole was susceptible to collapse under design loads.

It should also be noted that this project did not attempt to measure the fracture resistance of the tube. Since each of the tests was able to attain the cracked plastic moment capacity, the tube must have had adequate fracture resistance to the approximately 12-inch-long fatigue cracks.

**Table 6. Static testing matrix.**

Test	Specimen Designations	Crack Length Estimate (inches)	Temperature (°F)	Loading Rate (inch/s)	Peak Moment (kip-inch)
1	2G4	12.48	70	0.002	3,311 <sup>a</sup>
	2G6	11.42			
2	2G2	12.68	70	0.04	3,410 <sup>a</sup>
	2G1	13.77			
3	2G5	12.64	-30	0.02	3,342 <sup>a</sup>
	2G3	13.56			
4	2B5	11.76	-30	0.2	3,566 <sup>b</sup>
	2B6	12.61			

<sup>a</sup> Specimens have a full-section plastic moment capacity of 5,353 kip-inch ( $Z = 80.01 \text{ inch}^3$ ).

<sup>b</sup> Specimens have a full-section plastic moment capacity of 5,017 kip-inch ( $Z = 80.01 \text{ inch}^3$ ).

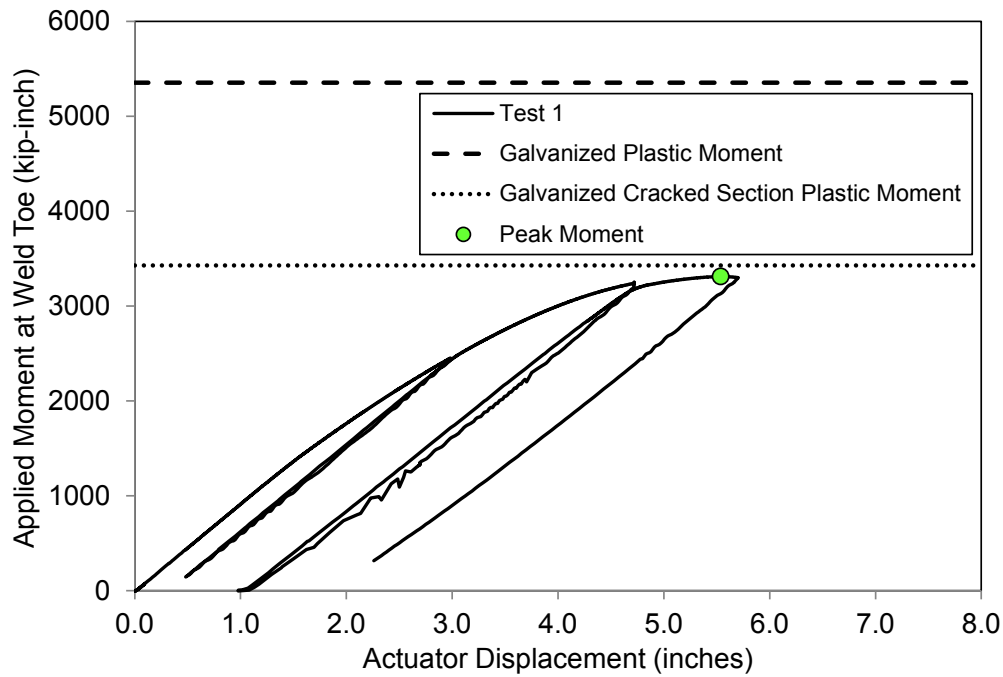


**Figure 7. Graph. Moment versus displacement of test 1.**

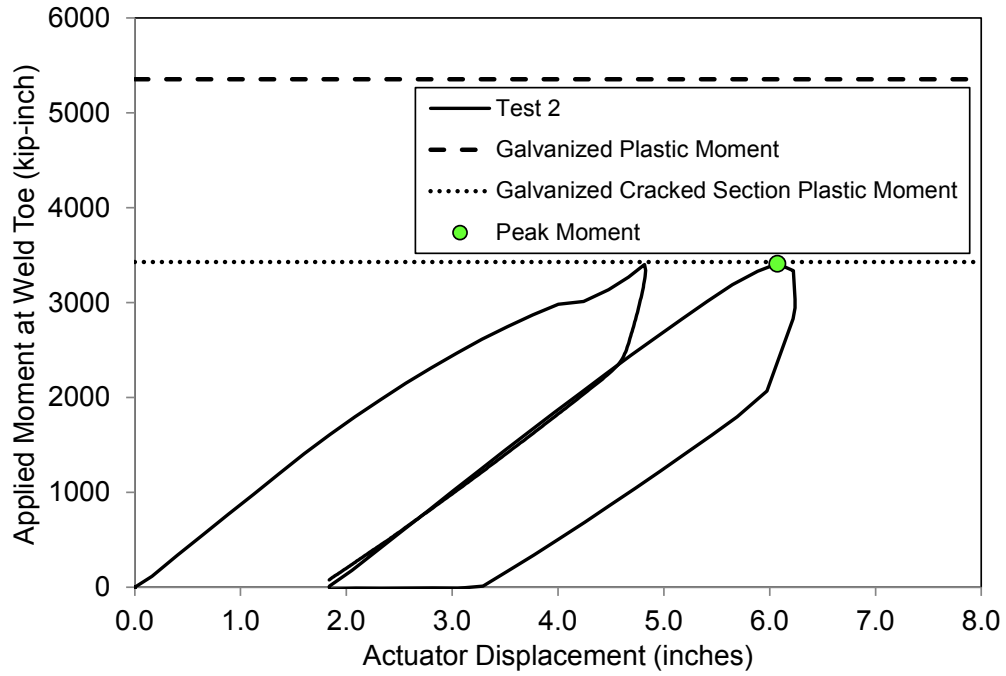


**Figure 8. Graph. Moment versus displacement of test 2.**

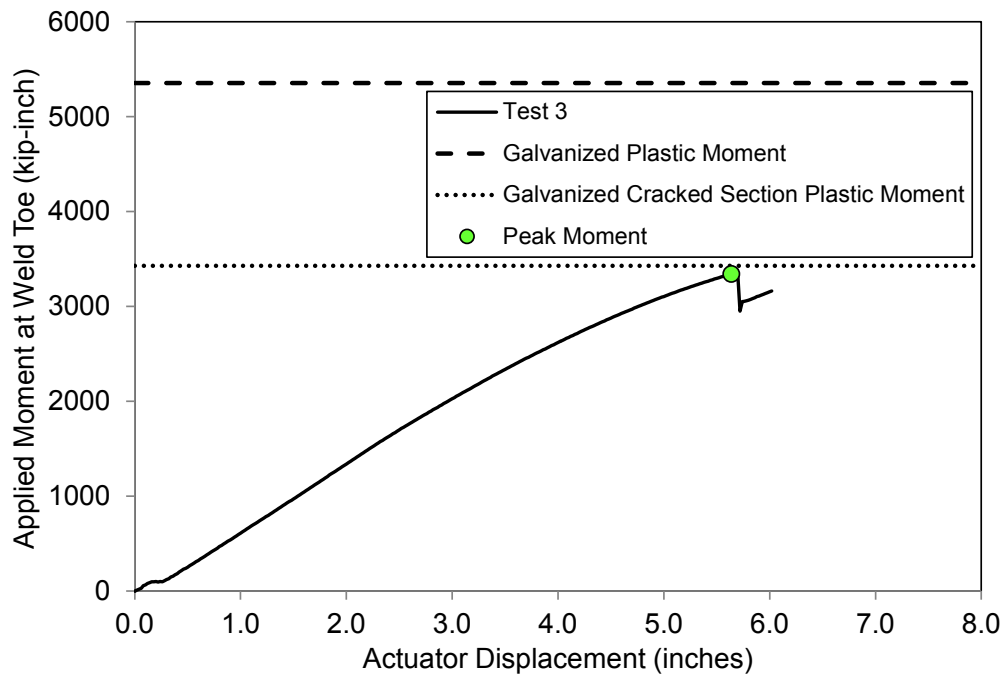


**Figure 9. Graph. Moment versus displacement of test 3.**

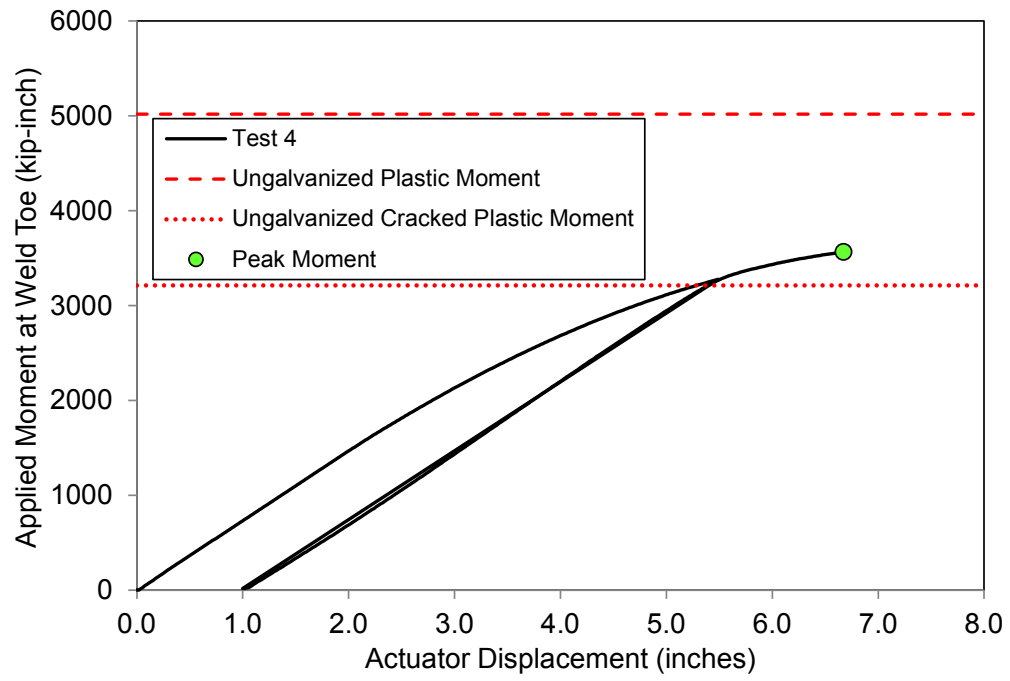


**Figure 10. Graph. Moment versus displacement of test 4.**



## SUMMARY

The fatigue tests on specimens from fabricator 1 showed how workmanship greatly influences the fatigue strength of socket connections and may govern over any effect galvanizing may have. The tests revealed that the poor performing welds had equal legs with undercuts, while the better performing welds had unequal legs and evidence of peening. This may speak to larger issues of quality control or the need for industry specifications for fatigue control in sensitive structures.

The test data from fabricator 2 show a pronounced difference in fatigue strength between galvanized and ungalvanized specimens, with galvanizing producing about a one category fatigue life reduction. However, current AASHTO specifications do not recognize the increase in fatigue life of ungalvanized specimens, and most of the fatigue data used to create the specifications were based on galvanized specimens.

Both sets of fatigue test data showed the galvanized specimens had a resistance much less than Category E'; however, the new AASHTO *Standard Specifications for Structural Supports for Highway Signs, Luminaires, and Traffic Signals*, 6th edition, still predicts the tested geometries have Category E' resistance.<sup>(11)</sup> There still appears to be a disparity in the new specifications, either in the determination of allowable stress range or in the workmanship standards to which these structures are fabricated.

A plastic cracked section analysis can accurately assess the remaining moment capacity of poles with cracks. To implement this analysis, one should also demonstrate confidence in the fracture toughness of the plate material. This project did not evaluate the fracture toughness, but except for one of the specimens, the fracture toughness was certainly high enough to sustain 12-inch-long cracks at temperatures to -30 °F.



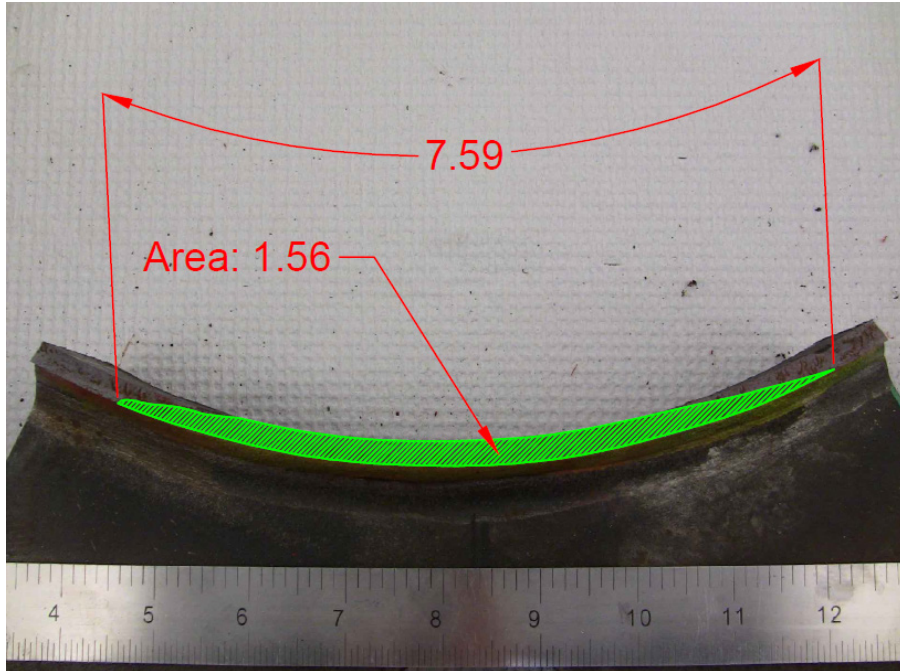


## APPENDIX: PICTURES OF FRACTURES

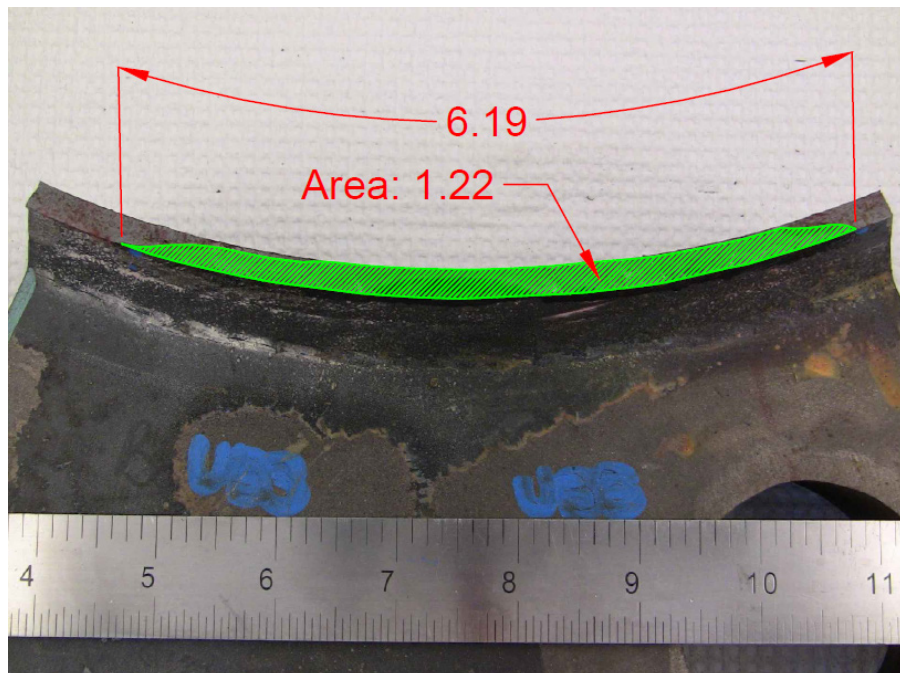
The pictures of the fracture surfaces shown in figure 11 through figure 33 are highlighted with green hatching to represent the area of fatigue crack growth. Two dimensions are provided for each hatched area: the length of the crack along the outer tube perimeter (in inches) and area of the crack (inches<sup>2</sup>).



Figure 11. Photo. Specimen 1U1 fracture surface.



**Figure 12. Photo. Specimen 1U2 fracture surface.**



**Figure 13. Photo. Specimen 1U3 fracture surface.**



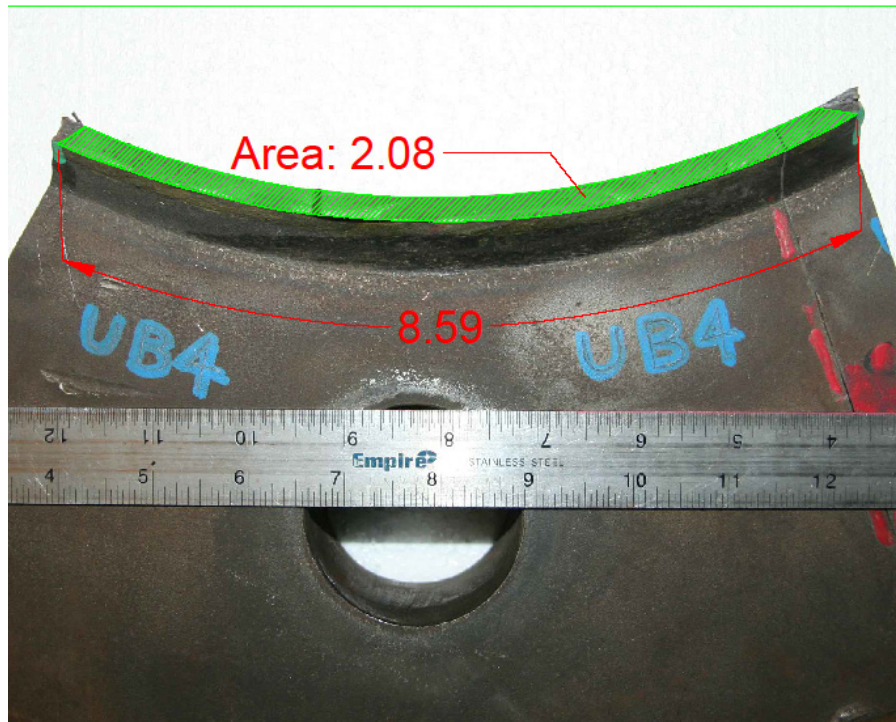


**Figure 14. Photo. Specimen 1U4 fracture surface.**

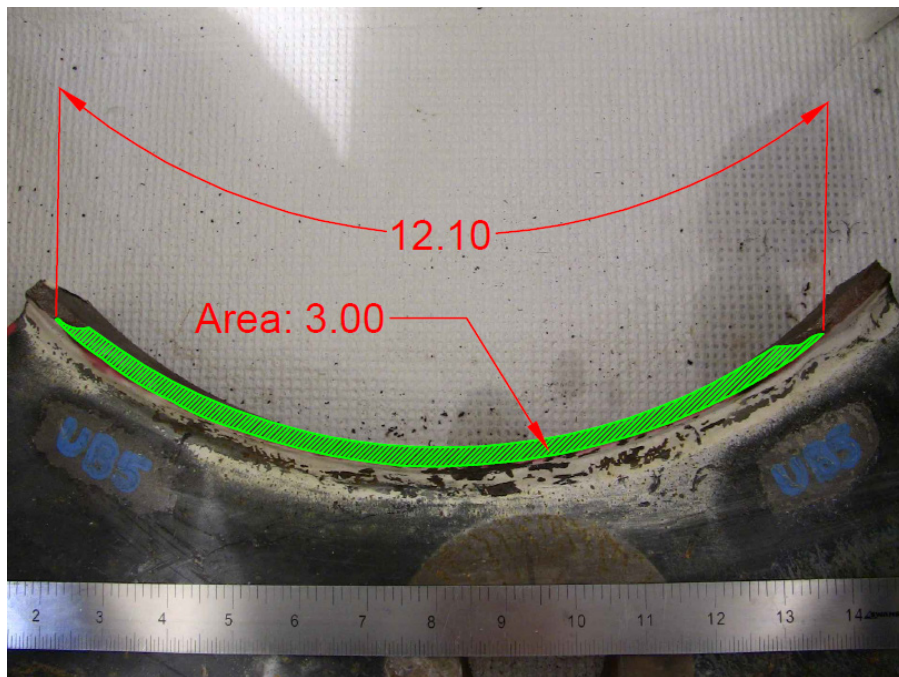


**Figure 15. Photo. Specimen 1U5 fracture surface.**

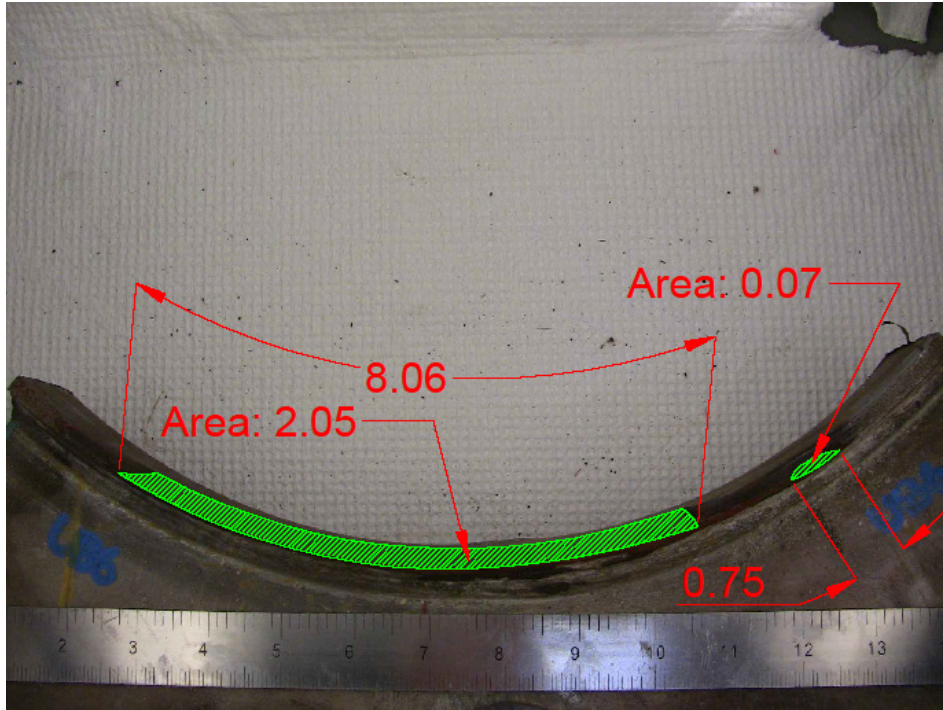


**Figure 16. Photo. Specimen 1U6 fracture surface.**

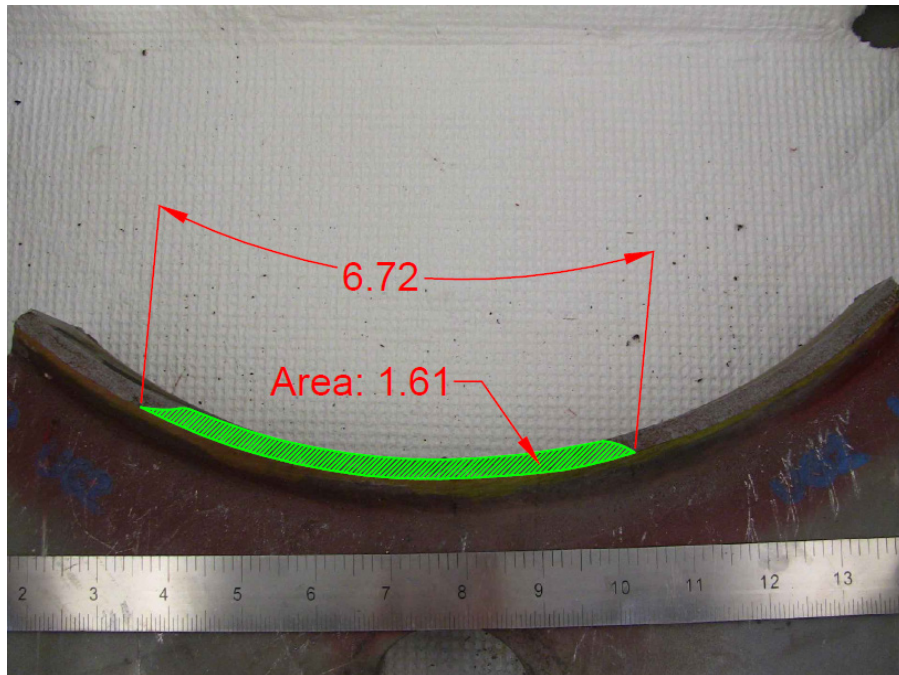


**Figure 17. Photo. Specimen 1G2 fracture surface.**



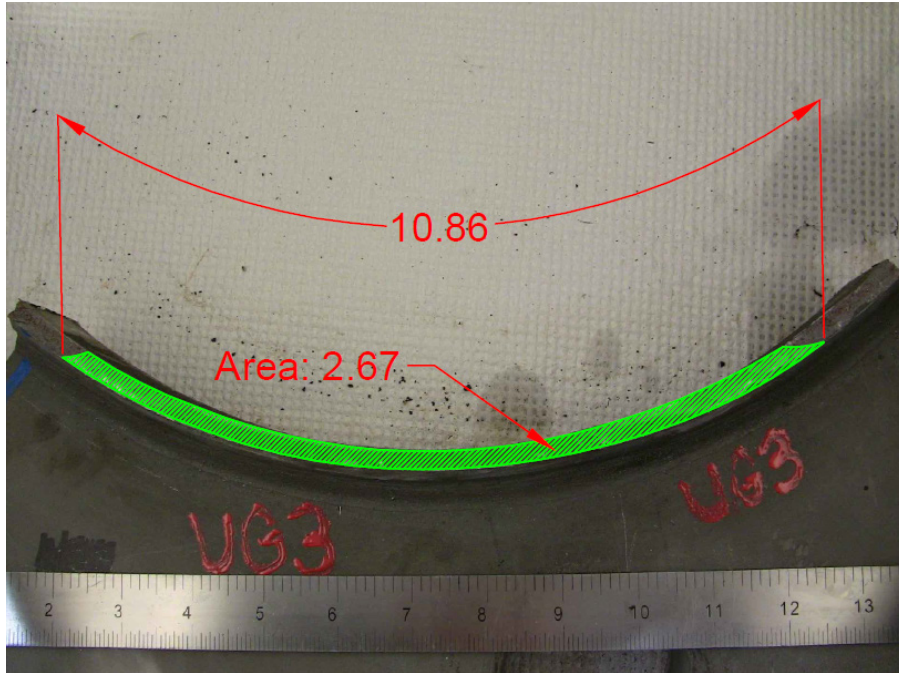


Figure 18. Photo. Specimen 1G3 fracture surface.

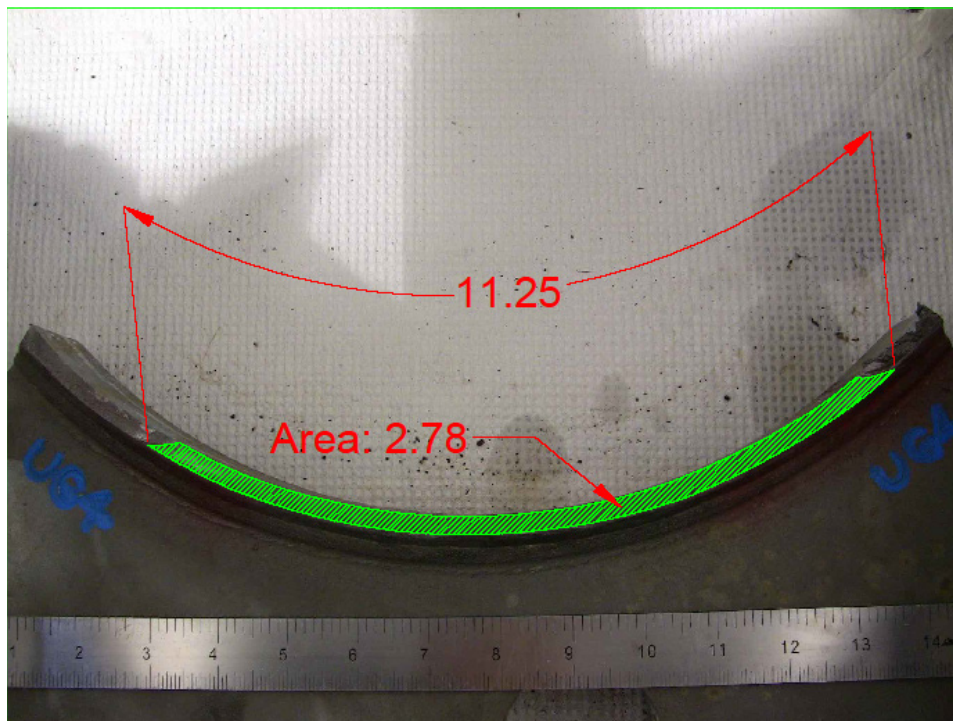


Figure 19. Photo. Specimen 1G4 fracture surface.

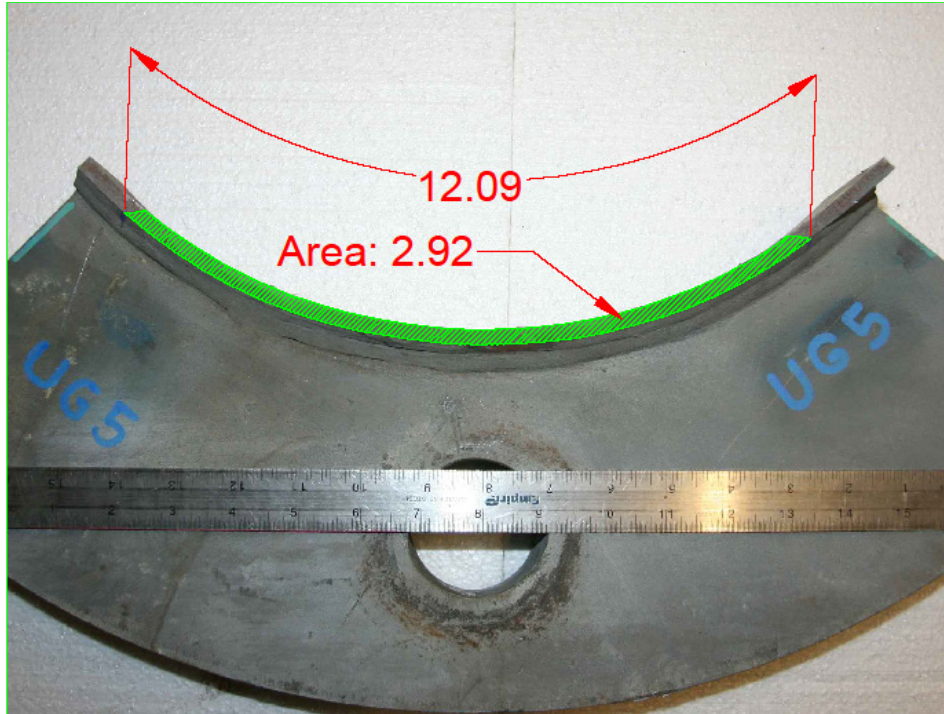


Figure 20. Photo. Specimen 1G5 fracture surface.

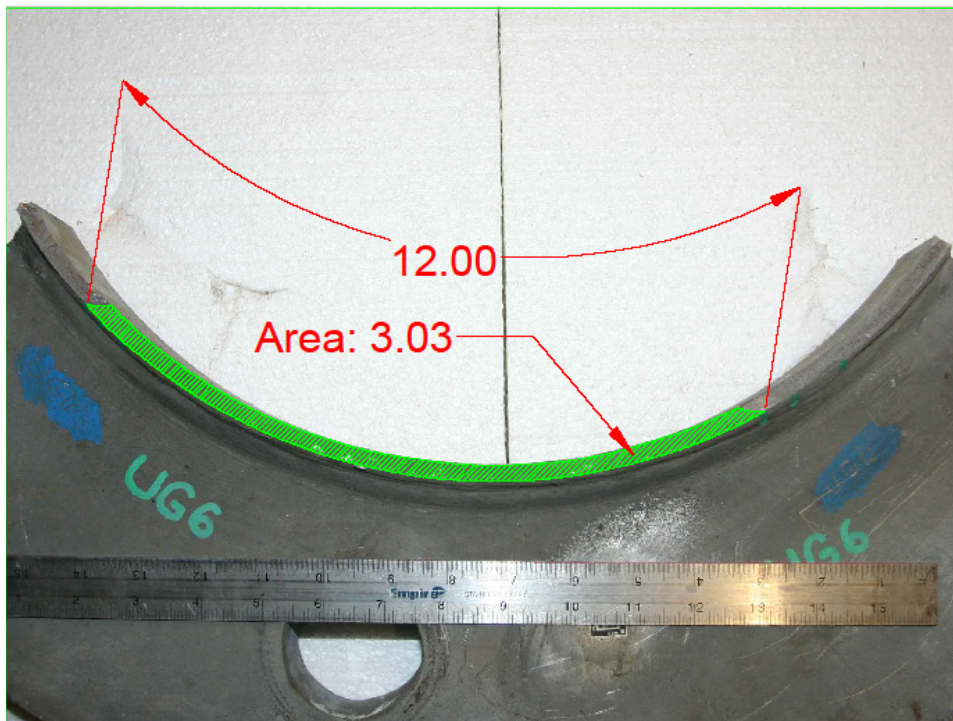
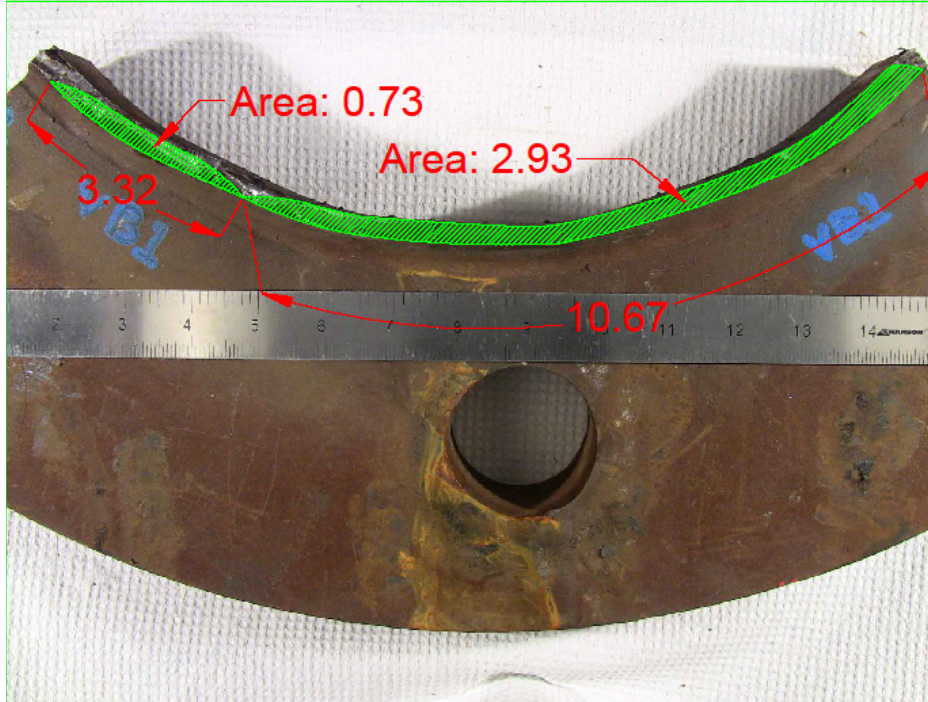
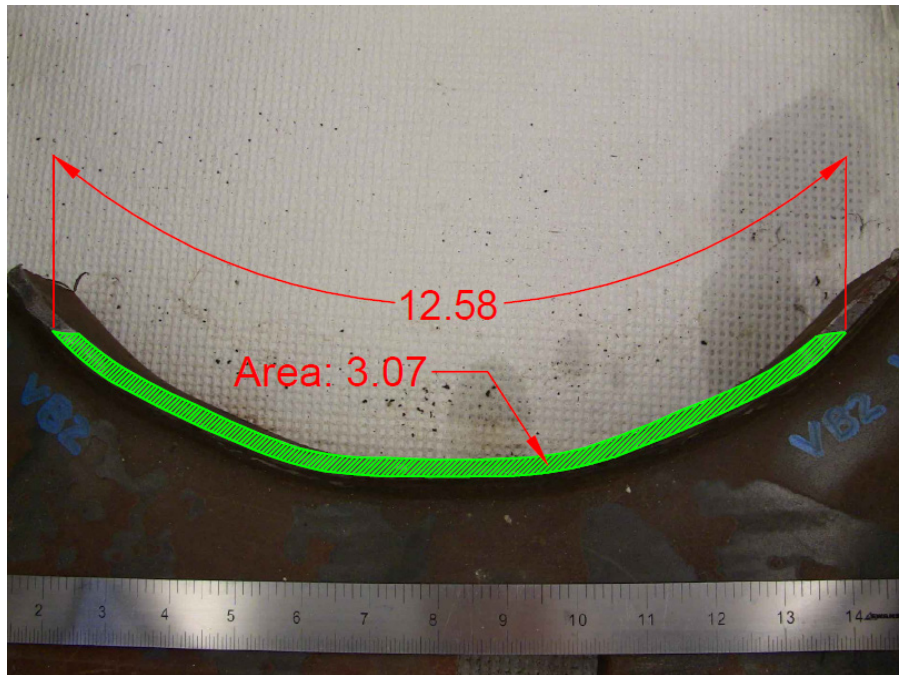


Figure 21. Photo. Specimen 1G6 fracture surface.





**Figure 22. Photo. Specimen 2U1 fracture surface.**



**Figure 23. Photo. Specimen 2U2 fracture surface.**

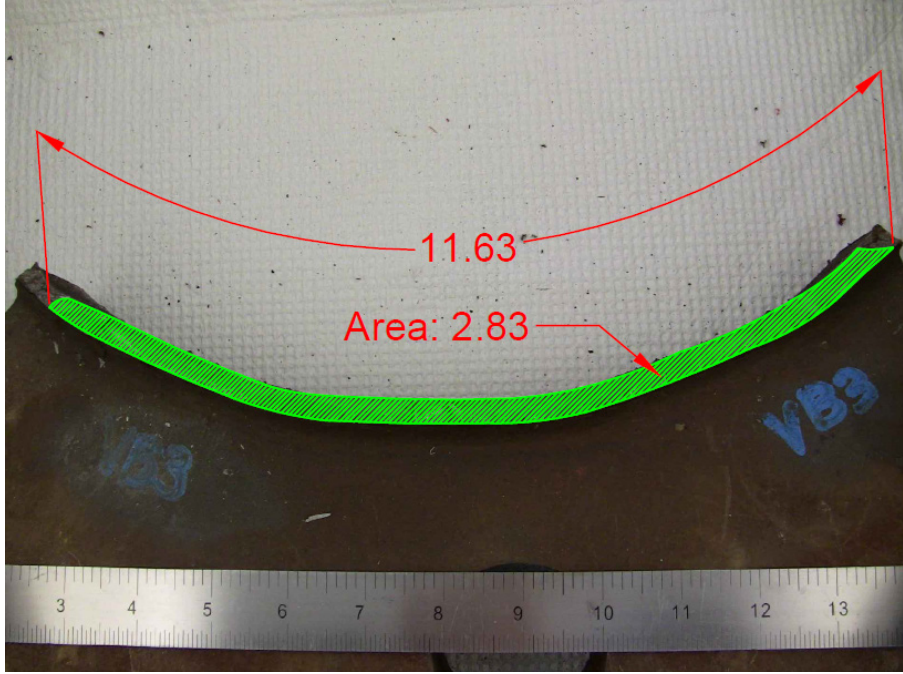


Figure 24. Photo. Specimen 2U3 fracture surface.

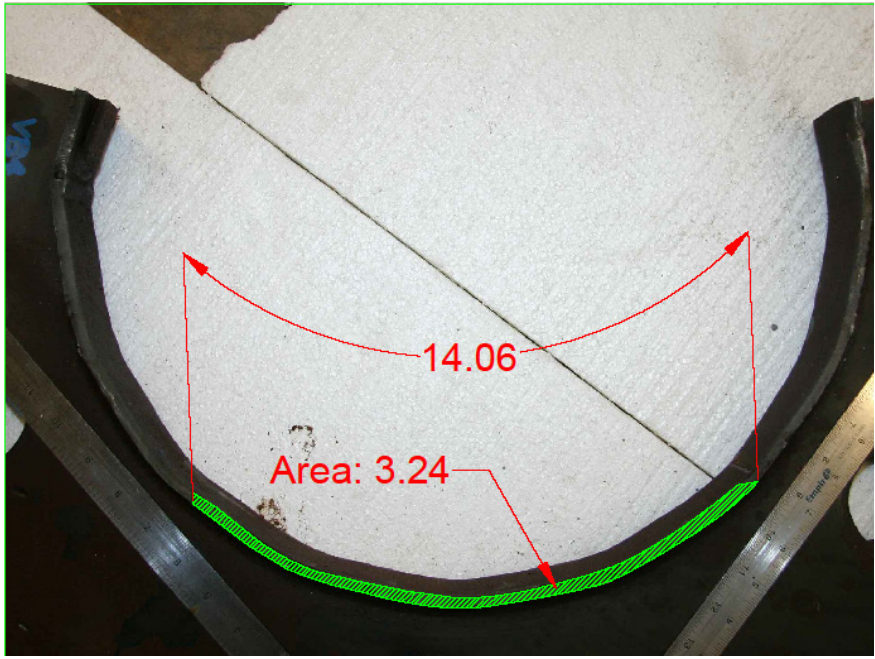
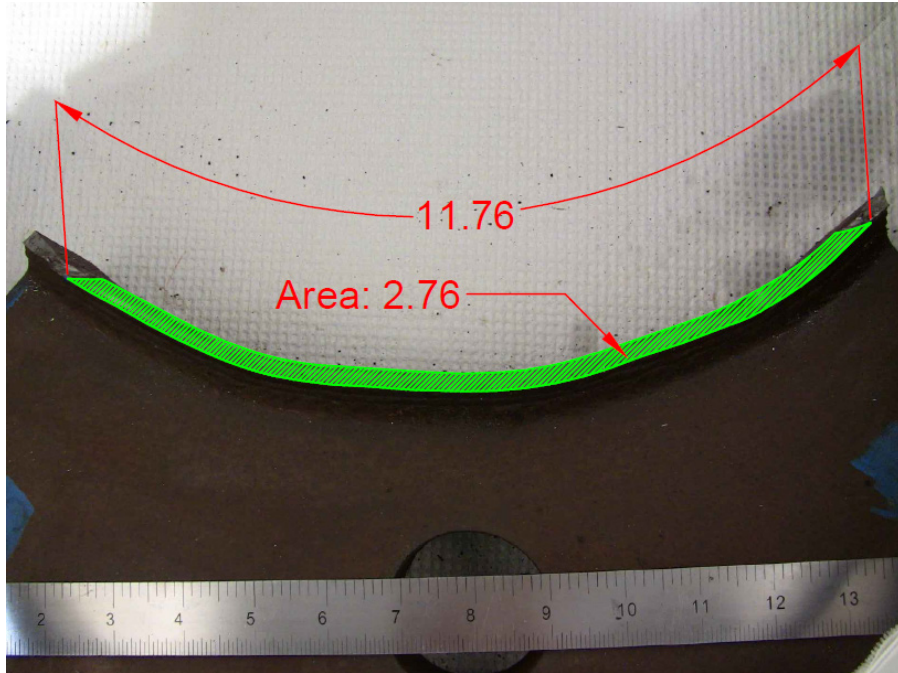
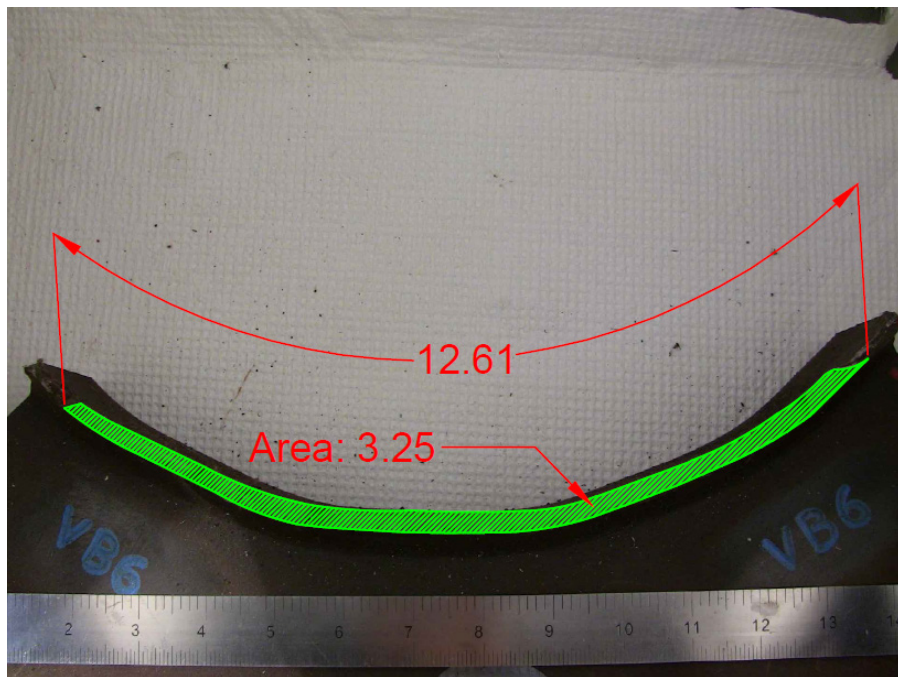


Figure 25. Photo. Specimen 2U4 fracture surface.





**Figure 26. Photo. Specimen 2U5 fracture surface.**



**Figure 27. Photo. Specimen 2U6 fracture surface.**

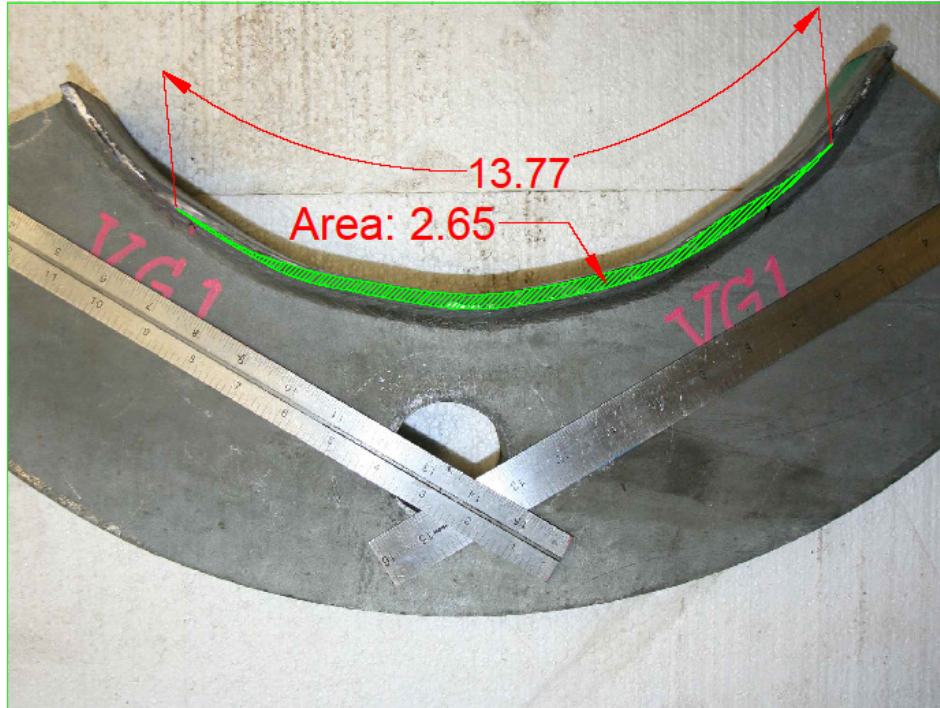


**Figure 28. Photo. Specimen 2G1 fracture surface.**

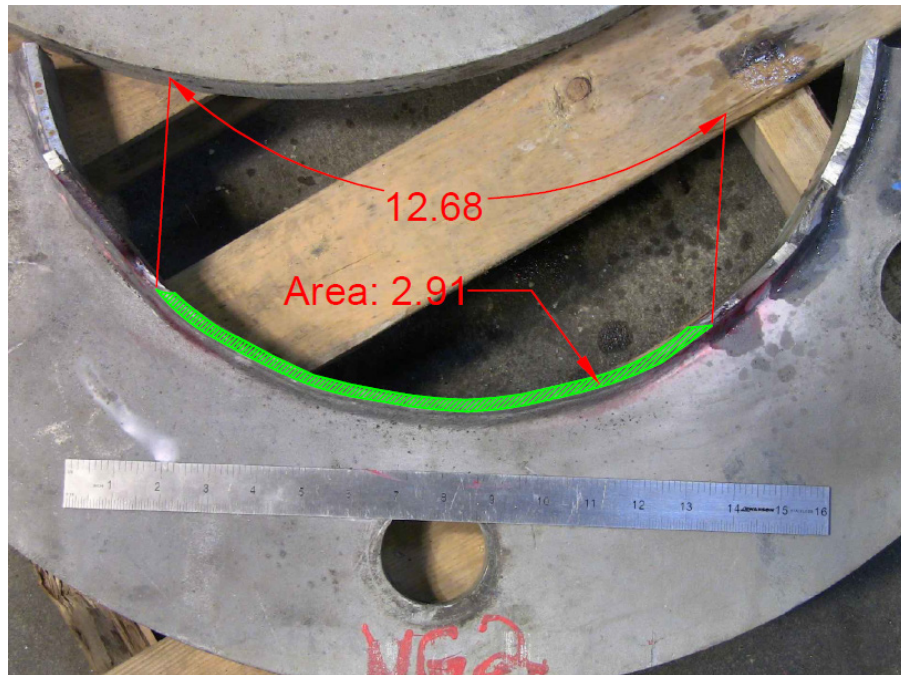


**Figure 29. Photo. Specimen 2G2 fracture surface.**



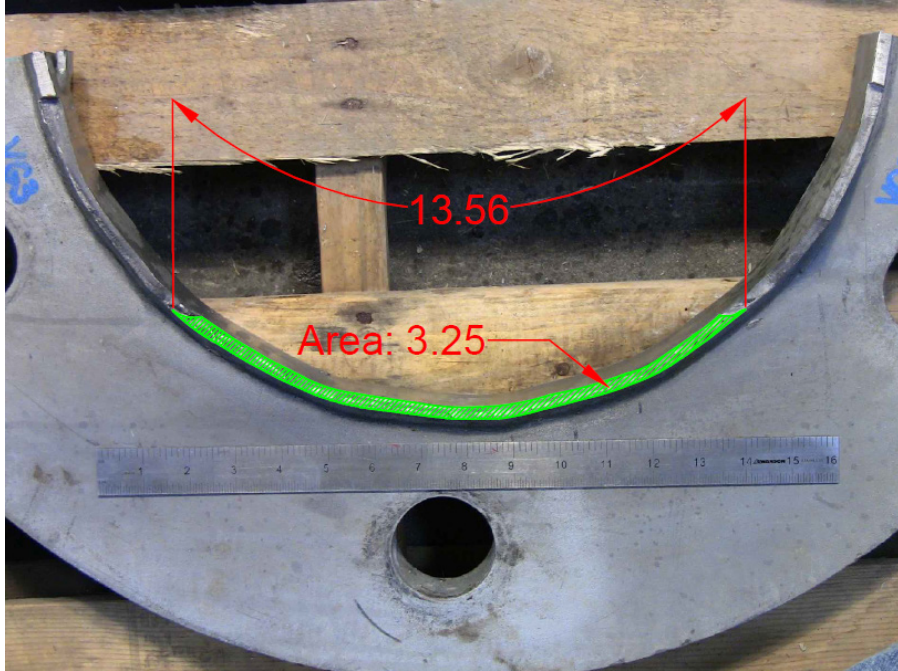


**Figure 30. Photo. Specimen 2G3 fracture surface.**

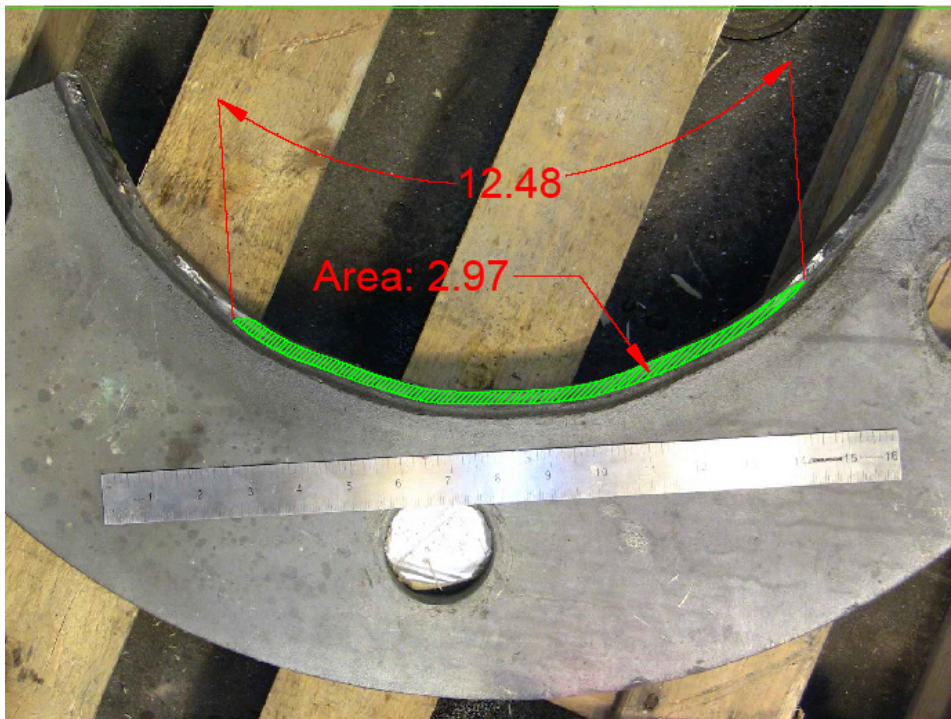


**Figure 31. Photo. Specimen 2G4 fracture surface.**

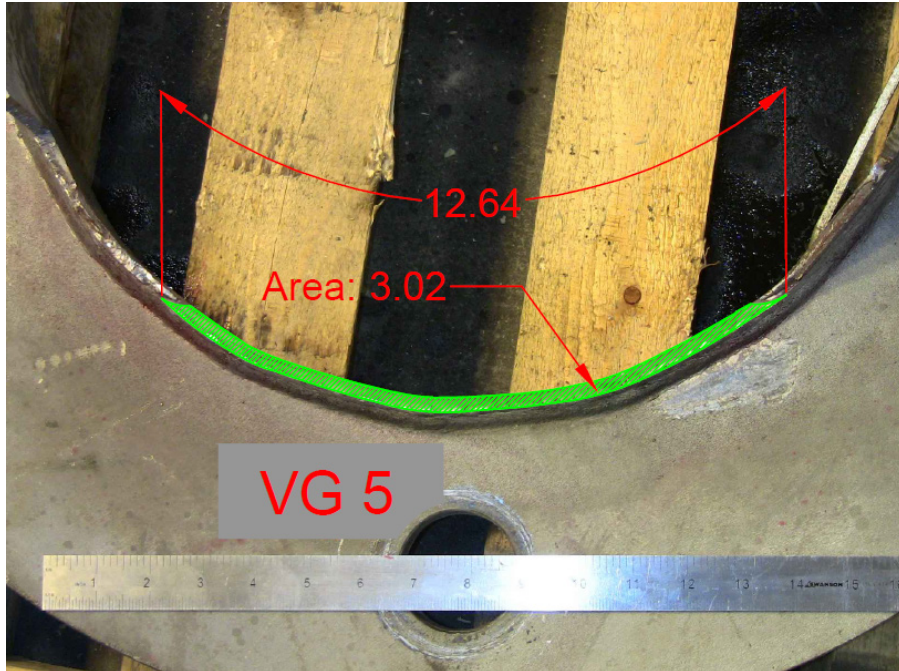


**Figure 32. Photo. Specimen 2G5 fracture surface.**

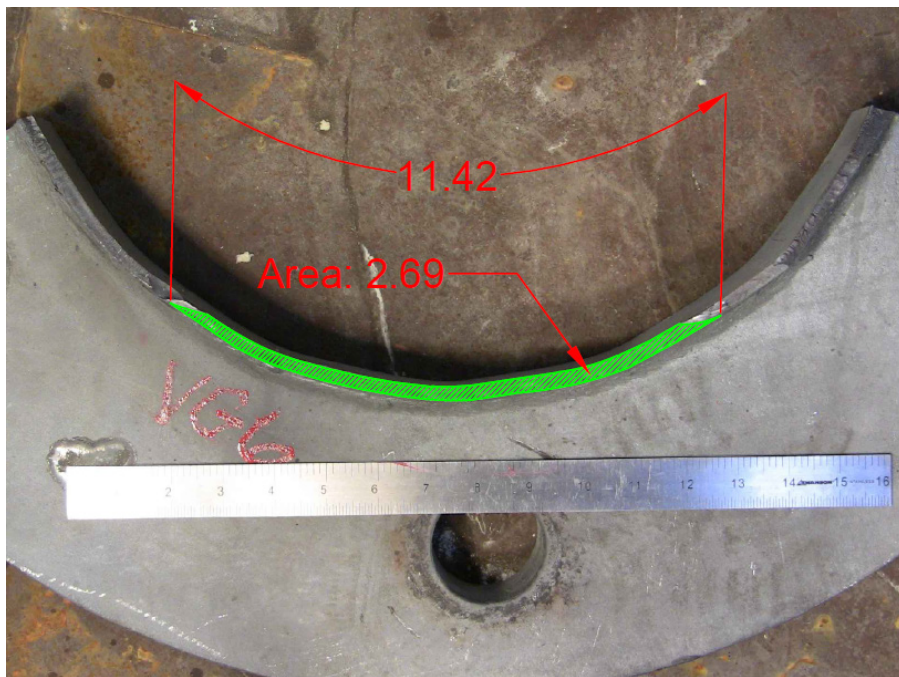


**Figure 33. Photo. Specimen 2G6 fracture surface.**

## REFERENCES

1. Culp, J. (1990). *Action Plan for Cantilever Sign Problem*, Report to Management, Michigan Department of Transportation, Lansing, MI.
2. Miki, C., J. Fisher, and R. Slutter (1981). *Fatigue Behavior of Steel Light Poles*, Lehigh University, Fritz Engineering Laboratory, Report No. 200.81.714.1, Bethlehem, PA.
3. AASHTO (2001). *Standard Specifications for Structural Supports for Highway Signs, Luminaires, and Traffic Signals*, 4th edition, American Association of State and Highway Transportation Officials, Washington, DC.
4. Hall, J.H. III (2005). *The Effect of Baseplate Flexibility on the Fatigue Performance of Welded Socket Connections in Cantilevered Sign Structures*, Master's Thesis, Lehigh University, Bethlehem, PA.
5. Hamilton, H.R., et al. (2004). *Traffic Signal Pole Research*, Wyoming Department of Transportation, Report No. FHWA-WY-04/03F, Laramie, WY.
6. Koenigs, M.T. (2003). *Fatigue Resistance of Traffic Signal Mast-arm Connection Details*, Master's Thesis, University of Texas, Austin, TX.
7. Ocel, J.M. (2006). *The Behavior of Thin Hollow Structural Section (HSS) to Plate Connections*, Ph.D. Dissertation, University of Minnesota, Minneapolis, MN.
8. Roy, S., et al. (2011). *Cost-Effective Connection Details for Highway Sign, Luminaire, and Traffic Signal Structures*, National Cooperative Highway Research Program Web-Only Document 176, Transportation Research Board, Washington, DC ([http://onlinepubs.trb.org/onlinepubs/nchrp/nchrp\\_w176.pdf](http://onlinepubs.trb.org/onlinepubs/nchrp/nchrp_w176.pdf)).
9. Stam, A., et al. (2011). *Fatigue Life of Steel Base Plate to Pole Connections for Traffic Structures*, Texas Department of Transportation, Report No. FHWA/TX-11/9-1526-1, Austin, TX.
10. ASTM E8-13 (2013). *Standard Test Methods for Tension Testing of Metallic Materials*, Book of Standards Volume 03.01, ASTM International, West Conshohocken, PA.
11. AASHTO (2013). *Standard Specifications for Structural Supports for Highway Signs, Luminaires, and Traffic Signals*, 6th edition. American Association of State and Highway Transportation Officials, Washington, DC.

